Book Section:
Butcher, F.E.G. orcid.org/0000-0002-5392-7286 (2022) Water ice at mid-latitudes on Mars. In: Oxford Research Encyclopedia of Planetary Science. Oxford Research Encyclopedias . Oxford University Press . ISBN 9780190647926

https://doi.org/10.1093/acrefore/9780190647926.013.239

Water Ice at Mid Latitudes on Mars

Frances E. G. Butcher[1]

[1]Department of Geography, The University of Sheffield, Winter Street, Sheffield, S10 2TN

Summary

Mars' mid latitudes, corresponding approximately to the 30–60° latitude bands in both hemispheres, host abundant water ice in the subsurface. Ice is unstable with respect to sublimation at Mars' surface beyond the polar regions, but can be preserved in the subsurface at mid-to-high latitudes beneath a centimetres-to-metres-thick covering of lithic material. In Mars' mid latitudes, water ice is present as pore ice between grains of the martian soil (termed 'regolith'), and as deposits of excess ice exceeding the pore volume of the regolith. Excess ice is present as lenses within the regolith, as extensive layers tens to hundreds of metres thick, and as debris-covered glaciers with evidence of past flow. Subsurface water ice on Mars has been inferred indirectly using numerous techniques including numerical modelling, observations of surface geomorphology, and thermal, spectral, and ground-penetrating radar analyses. Ice exposures have also been imaged directly by orbital and landed missions to Mars. Shallow pore ice can be explained by the diffusion and freezing of atmospheric water vapour into the regolith. The majority of known excess ice deposits in Mars' mid latitudes are, however, better explained by deposition from the atmosphere (e.g., via snowfall) under climatic conditions different from the present day. They are thought to have been emplaced within the last few million to 1 billion years, during large-scale mobilisation of Mars' water inventory between the poles, equator and mid-latitude regions under cyclical climate changes. Thus, water ice deposits in Mars' mid latitudes probably host a rich record of geologically-recent climate changes on Mars. Mid-latitude ice deposits are leading candidate targets for *in situ* resource utilisation of water ice by future human missions to Mars, which may be able to

sample the deposits to access such climate records. *In situ* water resources will be required for rocket fuel production, surface operations, and life support systems. Thus, it is essential that the nature and distribution of mid-latitude ice deposits on Mars are characterised in detail.

Keywords

Mars, Ice, Water, Climate, Glaciers, In Situ Resource Utilisation.

Introduction

Mars is an icy planet. Its polar ice caps were studied by 17th–20th century observers using ground-based telescopes (e.g., Herschel, 1784). Advancements in Mars observation (including the first flybys, orbital missions, and landings) during the second half of the 20th century revealed that Mars' middle and high latitude regions also host water ice (Figure 1) in the subsurface, potentially in volumes equivalent to a global layer of water several metres deep (e.g., Head et al., 2003; Levy et al., 2014).

In the present day, perennial water ice cannot exist at the surface equatorward of Mars' polar regions. This is because, for a significant portion of the martian year, surface temperatures exceed the sublimation point of water ice under Mars' low atmospheric pressure (~6 mbar on average). Above the sublimation point, ice transitions straight to a gas without passing through the liquid phase. Therefore, any seasonal water ice frost that accumulates at the surface in winter sublimates back into the atmosphere in spring. However, a centimetres-to-metres-thick covering of lithic material (dependent on latitude and local surface properties) can inhibit sublimation sufficiently to allow perennial stability of ice in the subsurface. The focus of this article is on subsurface water ice in Mars' mid-latitude regions, corresponding approximately to the regions between ~30–60° latitude in the northern and southern hemispheres.

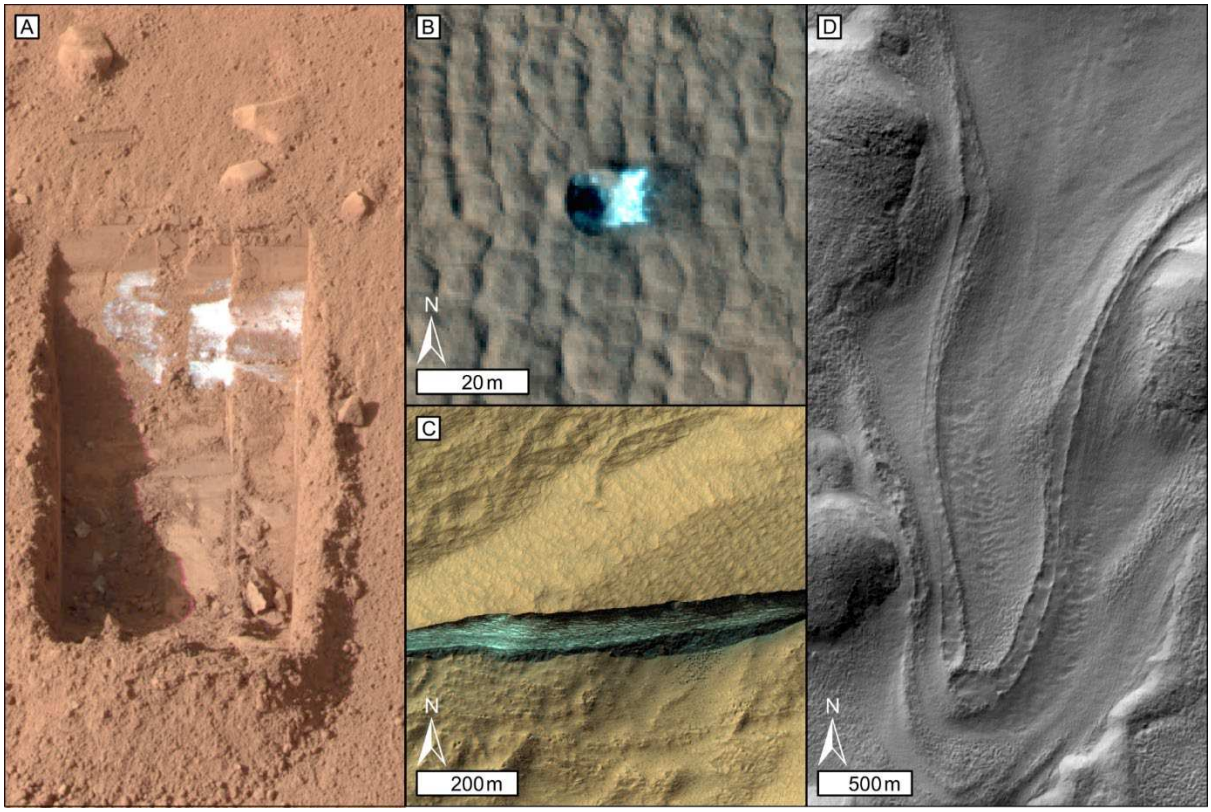

Figure 1: Examples of some of the non-polar ice deposits that will be discussed in this article. *(A) Phoenix Lander image of subsurface water ice in a ~15 cm-wide trench, which it excavated at ~68°N. After Mellon et al. 2009. (B) Orbital image of subsurface water ice exhumed by a small, fresh impact crater at ~46°N, identified by Byrne et al. (2009). High Resolution Imaging Science Experiment (HiRISE) false colour image ESP_011494_2265. (C) Orbital image of a scarp identified by Dundas et al. (2018), exposing a hundred-metre-thick layer of buried water ice at 58.1°S. HiRISE false colour image ESP_040772_1215. (D) Orbital image of a 'glacier-like form' thought to have formed by the flow of debris-covered glacial ice at 38°S. After Milliken et al. (2003). Mars Orbiter Camera image M1800897.*

Image credits: F. Butcher with data from: (A) NASA/JPL/University of Arizona/Texas A&M University. (B) and (C) NASA/JPL/University of Arizona. (D) NASA/JPL/Malin Space Science Systems. MOC image: Malin, K. S. Edgett, S. D. Davis, M. A. Caplinger, E. Jensen, K. D. Supulver, J. Sandoval, L. Posiolova, and R. Zimdar, M1800897, Malin Space Science Systems

Mars Orbiter Camera Image Gallery (http://www.msss.com/moc_gallery/), Release date: 4 April 2001

Water ice exists in the subsurface in Mars' mid latitudes as pore ice between regolith grains, and as segregated deposits of relatively pure excess ice. Excess ice exists as: lenses within the martian soil (e.g., Figure 1A); thicker, more extensive layers up to hundreds of metres thick (e.g., Figure 1C); and as debris-covered glaciers with evidence for past flow (e.g., Figure 1D). These ice deposits are thought to have been emplaced at various times within the last 1 billion years, recording large-scale mobilisation and redistribution of Mars' water inventory in response to relatively recent, cyclical climate changes.

Motivations for Study

Mars research has long been motivated by the search for water and its implications for palaeoclimate and habitability. The prediction and subsequent discovery of widespread subsurface water ice during the second half of the 20th century was, therefore, intriguing. Much interest in Mars' mid-latitude ice deposits has been on their distribution, the nature and environmental drivers of their deposition and evolution; the volume of ice they contain; and their implications for the availability of water earlier in Mars' history. Mars' known mid-latitude ice deposits are thought to have been emplaced as a result of cyclical climate changes during Mars' most recent geologic period: the 'Amazonian'. These climate changes are thought to have occurred long after the main period of water activity on Mars (the Noachian period, >3.7 billion years ago), generating features with modelled ages ranging from <1 million, to hundreds of millions of years. Therefore, it is likely that Mars' mid-latitude ice deposits contain records which could be used to reconstruct complex variations in palaeoenvironmental conditions in Mars' recent geologic history.

Subsurface ice deposits are protected from the harsh radiation environment at Mars' surface, and landforms associated with them have raised the question of whether they have ever produced meltwater, which is considered essential for life. Therefore, mid-latitude ice deposits are also of interest in the search for recently-habitable environments on Mars (e.g., Cabrol, 2021).

Water ice deposits in Mars' mid latitudes are also prime targets for *in situ* resource utilisation by future crewed missions to the surface of Mars (e.g., Morgan et al., 2021; Putzig et al., Submitted). Human missions to Mars will require *in situ* water resources for vital systems, including rocket fuel production. While the polar caps contain abundant water ice, they are unlikely to provide suitable landing sites for early crewed missions. Greater insolation and less extreme environmental conditions at Mars' mid latitudes have made these regions more favourable for crewed exploration than the martian poles.

Evolution of Studies

Early Hypotheses of Mid-Latitude Water Ice on Mars

Early suggestions that Mars' non-polar regions host buried ice emerged from attempts to explain light and dark areas observed on Mars' surface from ground-based telescopes (e.g., Baumann, 1909; Lederberg & Sagan, 1962). Vegetation was thought to be one viable explanation for these features, and ground ice was considered as a potential source of water to sustain it (Lederberg & Sagan, 1962; Salisbury, 1966; Strughold, 1967). However, data returned during the Mariner program (e.g. Leighton et al., 1965, 1969; McCauley et al., 1972; Sagan et al., 1972), which included the first flyby of Mars by Mariner 4 in 1965 (Leighton et al., 1965; Kliore et al., 1965), demonstrated that Mars hosts a harsh, barren surface environment, and that inorganic processes provided better explanations for the light and dark

areas (e.g., Sagan et al., 1972). This negated the requirement for non-polar water ice to sustain vegetation, but the distribution of ices on Mars remained a topic of significant interest.

Theoretical Predictions of Ground Ice after the 1965 Mariner 4 Flyby of Mars

Enduring theories on the nature and distribution of water ice in Mars' mid latitudes emerged following the first flyby of Mars by NASA's Mariner 4 spacecraft. Mariner 4 observations of Mars' atmosphere (Kliore et al., 1965) suggested that, at mid-to-high latitudes, water vapour in the atmosphere would tend to diffuse into the pore space within the martian soil (termed 'regolith') and freeze as ground ice (Leighton & Murray, 1966). Based on thermal modelling, Leighton and Murray (1966) predicted the presence of perennial ground ice in areas where the annual mean vapour pressure in the subsurface was in equilibrium with the atmosphere, corresponding to regions poleward of 40–50°N/S. Leighton and Murray (1966) predicted that the top of a perennial ice table was in the very shallow subsurface at high latitudes, deepening to 1–2 m depth towards the mid latitudes. At shallower depths above the perennial ice table, later described as the 'tempofrost' zone by Farmer and Doms (1979), ice would be unstable with respect to the atmosphere (at least seasonally), and any seasonal ice deposited during the winter (e.g. as frost) would be lost to the atmosphere by sublimation during the warmer seasons. At lower latitudes, ice would be unstable at depth unless vapour diffusion to the atmosphere was inhibited by overlying materials. Several refinements to the modelled depth, nature, and distribution of mid-latitude ice (and its spatiotemporal variations) were made in the decades following the Leighton and Murray model (e.g., Fanale, 1976; Farmer & Doms, 1979; Rossbacher & Judson, 1981; Fanale et al., 1986; Mellon & Jakosky, 1993; Mellon et al., 2004). However, the fundamental theory has remained broadly similar. Figure 2 shows a schematic representation of this concept.

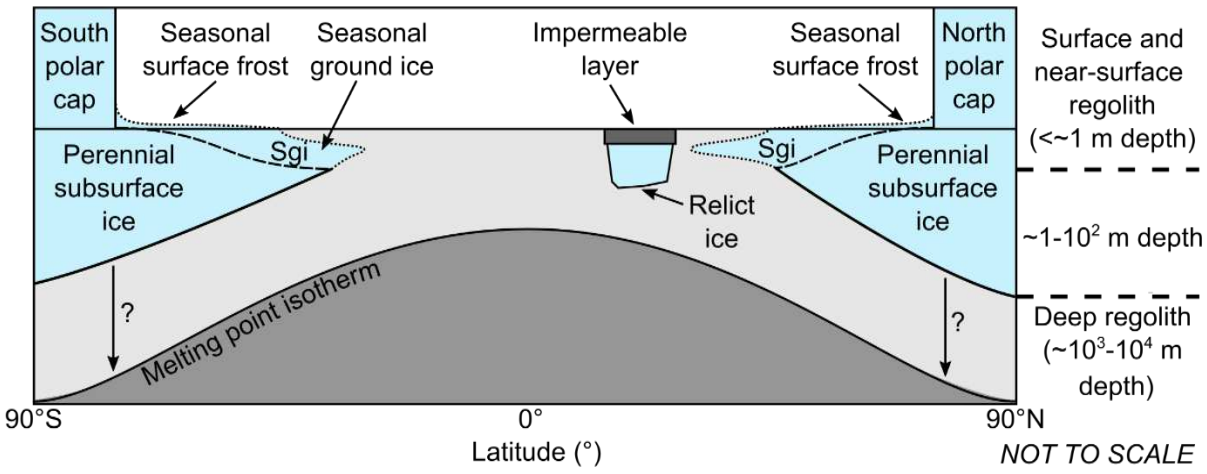

Figure 2: Schematic of the theoretical latitude distribution of present-day ice reservoirs on Mars. *The horizontal dashed lines (right) mark changes in vertical scale. Dotted lines delimit zones of seasonal ice stability. Note that water ice comprises a minor component of seasonal surface frosts, which are predominantly CO_2 ice. An example of relict ice that has been preserved due to isolation from the atmosphere is shown; such relict ice deposits exist in both hemispheres. This illustration represents a supply-limited scenario, where subsurface ice does not extend down to the melting point isotherm.*

Image Credit: Redrawn and modified by F. Butcher from Butcher (2019).

Theoretical Predictions of Ground Ice after the Viking Program

Mariner-era (and many Viking-era) numerical models of Mars' subsurface ground ice distribution focussed primarily upon latitudinal variations in the depth to the top of the ice table. They typically assumed uniform regolith properties across Mars' surface, and that the dominant process of ice emplacement was by vapour diffusion from the atmosphere (Leighton & Murray, 1966; Fanale, 1976; Farmer & Doms, 1979; Rossbacher & Judson, 1981; Fanale et al., 1986).

The subsequent generation of models, facilitated by more detailed observations from the Viking program, scrutinised the mid-latitude ground ice distribution in more dimensions. For

example, Mellon and Jakosky (1993) predicted 20–30° variations in the latitudinal boundary of near-surface ice stability resulting from longitudinal variations in the thermal inertia and albedo of the regolith. The top of the ice table deepened and the boundary of the stable zone moved to higher latitudes within high thermal inertia/low albedo ice-free materials (Mellon & Jakosky, 1995; see also Paige, 1992).

Viking-era thermal models highlighted that water vapour from the atmosphere may only supply ground ice to depths of ~10 m, where geothermal heating from the planet's interior begins to dominate over annual temperature fluctuations at the surface (e.g., Clifford & Hillel, 1983; Clifford, 1991; Mellon & Jakosky, 1993). Water vapour at greater depths would tend to diffuse upwards towards the surface along the geothermal gradient, thus inhibiting thickening of an ice layer derived directly from diffusion from the atmosphere. This did not, however, mean that ice was absent at greater depth. Mechanisms proposed for the emplacement of ice beyond the shallow zone of vapour diffusion from the atmosphere included: (1) freezing of groundwater sourced from depth (Clifford, 1991; Mellon & Jakosky, 1993), and/or (2) the deep burial of surface ice deposits (e.g., Mellon & Jakosky, 1993).

Another dimension to explore was that of time. How long would it take for vapour diffusion to emplace and remove near-surface ground ice, beyond depths influenced by seasonal temperature variations? How could deposits (whether emplaced by vapour diffusion or other mechanisms) be affected by cyclical climate changes induced by variations in Mars' obliquity (its axial tilt) and the eccentricity of its orbit (i.e., how elliptical the orbit is) over the last few million years? Mellon and Jakosky (1995) adapted their earlier model (Mellon & Jakosky, 1993) to include insolation variations driven by a model varying planetary obliquity and eccentricity. They found that obliquity, which they modelled to have varied between 15° and 35° during ~100 kyr cycles, exerted the most significant control on variations in near-surface ground ice distribution. During periods of high modelled obliquity, vapour diffusion from the

atmosphere generated stable ground ice deposits at all latitudes. In contrast, during periods of low modelled obliquity, ice was removed from the upper 1–2 m of the subsurface equatorward of 60–70° latitude (Mellon & Jakosky, 1995). Notably, however, deeper deposits in the mid latitudes survived through low obliquity intervals. Thus, the model demonstrated a long-term accumulation of shallow ground ice in the mid latitudes, and that ice could survive in these regions in the present day as relicts of a past climatic regime. At more equatorial latitudes <30°N/S, all ice deposited during a given high-obliquity excursion was removed during the subsequent low-obliquity episode, and the regolith became desiccated (Mellon & Jakosky, 1995).

Observations of Ice-Related Landforms by the Mariner and Viking Missions

The data returned from the Mariner missions to Mars, and later the Viking orbiters and Viking 2 lander (Mutch et al., 1977; Snyder, 1979), provided hints that subsurface water ice is indeed present in Mars' mid latitudes, and has played a significant role in the modification of the landscape.

'Terrain Softening' by Mantling Deposits.

In a planet-wide survey using Mariner 9 images, Soderblom et al. (1973) tentatively identified latitude-dependent blankets of material (termed 'mantle') which draped terrain poleward of ~30° in each hemisphere. They suggested that these deposits comprised debris transported by wind from the polar regions. The involvement of ice was later suggested on the basis of Viking orbiter images (Carr & Schaber, 1977; Squyres & Carr, 1986). A global survey conducted by Squyres and Carr (1986) revealed that, in places, the deposits appeared to have convex slopes, rather than the concave slopes that would be expected by windblown deposits draping topography. They argued that the deformation of ice derived from atmospheric vapour diffusion into the deposits offered a better explanation. Data from the late 1990s onwards, however, suggests that ice in these latitude-dependent mantling deposits was derived from

climatically-driven cycles of dust and snow deposition in Mars' mid-to-high latitudes, rather than vapour diffusion into near-surface layers (e.g., Head et al., 2003).

Ice-Rich Viscous Flow Features

Another notable early observation from Mariner 9 images was of deposits within broad, steep-sided valleys in Mars' northern mid latitudes (Sharp, 1973). More extensive, higher-resolution (decametre-scale) imaging by the Viking orbiters (Figure 3) revealed that these features were deposits with lineated surface morphologies suggestive of ice-assisted flow of materials along valley floors and away from steep slopes (Squyres, 1978, 1979). The observed features had lengths of tens of kilometres and thicknesses of hundreds of metres, and occurred within ~25°-wide latitude bands centred around 40°N and 45°S (Squyres, 1978, 1979; Squyres & Carr, 1986). The latitudinal pattern of their distribution suggested some climatic control on the supply of ice. Where these deposits filled valleys, they were named 'lineated valley fill' (Figure 3A); where they extended from the base of isolated hills and mesas, they were named 'lobate debris aprons' (Figure 3B–C); and where they infilled impact craters, they were named 'concentric crater fill' (Figure 3D; Squyres, 1978, 1979).

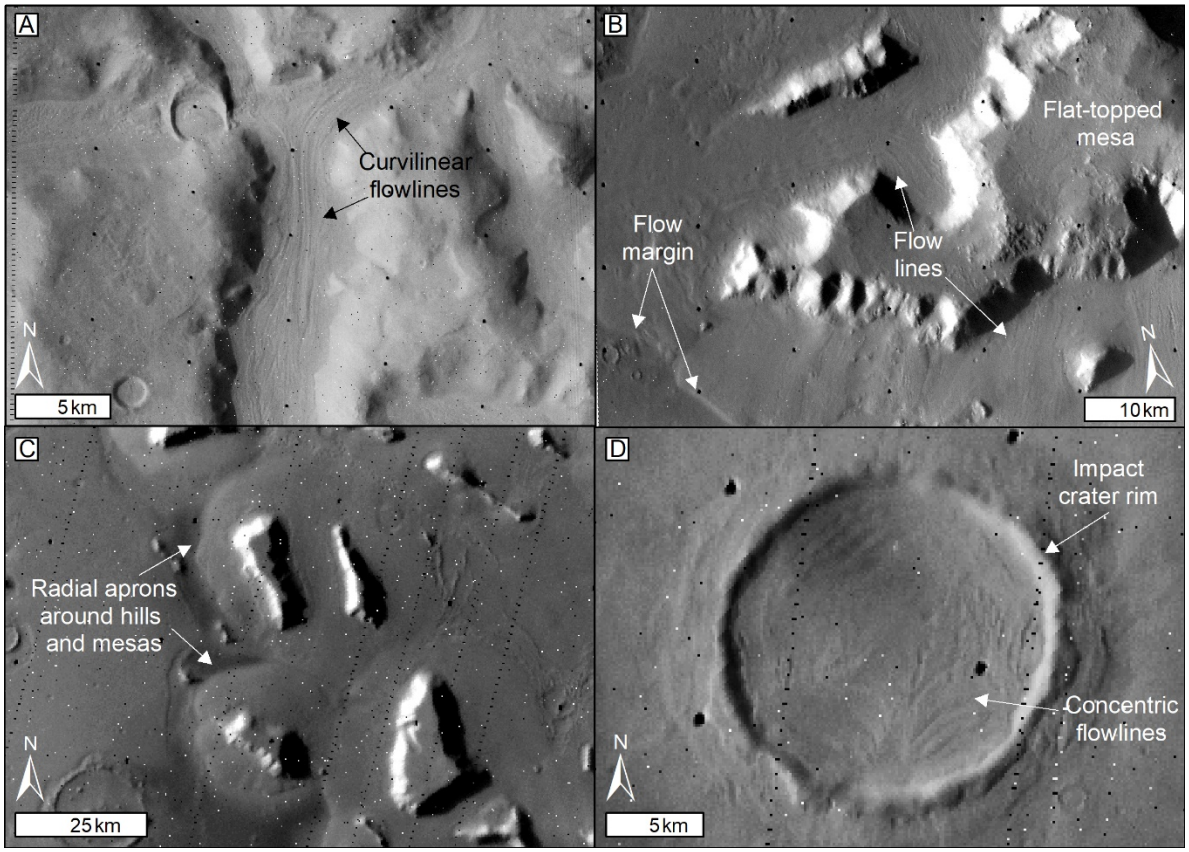

Figure 3: Viking Orbiter Images of Ice-Rich Viscous Flow Features. *Illumination from left in all images. (A) Lineated valley fill at ~33.6°N. Viking orbiter image 84A73. (B) Lobate debris aprons extending from a flat-topped mesa at ~45°N. Faint flowlines are visible on the surfaces of the features. Viking orbiter image 58B55. (C) Lobate debris aprons extending radially from isolated mesas at ~44°N. Viking orbiter image 675B42. (D) Concentric crater fill filling an impact crater at 41.5°N, and hosting concentric flowlines on its surface. The black dots are not real surface features. Viking orbiter image 10B70.*

Image credit: F. Butcher, with data from NASA/JPL.

Most Mariner and Viking-era studies suggested that these viscous flow features comprised bulk debris derived from adjacent hillslopes, and <50% (perhaps 10–30%) ice content by volume in between clasts (Sharp, 1973; Carr & Schaber, 1977; Squyres, 1978, 1979; Rossbacher & Judson, 1981). Multiple formation mechanisms involving ice-assisted flow were proposed,

including creep of ground ice (Sharp, 1973), ice-rich landslides (Lucchitta, 1984), ice-assisted debris flows (Rossbacher & Judson, 1981; Kochel & Peake, 1984), and rock glaciers (Squyres, 1978, 1979; Squyres & Carr, 1986). Data from early 21st century missions has called into question the debris content of these features, suggesting instead that they are debris-covered glaciers comprising bulk water ice covered by a thin (<10 m) layer of surficial debris (e.g., Head et al., 2005; Holt et al., 2008; Plaut et al., 2009; Petersen et al., 2018).

Scalloped Depressions interpreted as Thermokarst Terrain

Thermokarst terrain comprises surface depressions formed by the loss of segregated subsurface ice. Segregated (or 'excess') ice exceeds the pore space of the regolith (i.e. comprising >50% of its volume), and cannot be explained by vapour diffusion from the atmosphere alone. The formation of excess ice requires either migration of water through the substrate, or deposition by precipitation and subsequent burial. The existence of thermokarst terrain in Mars' mid latitudes was postulated on the basis of Mariner 9 images (e.g., Gatto & Anderson, 1975). While the thermokarst hypothesis did not endure for these specific features, more convincing thermokarst terrains were later identified from Viking orbiter images of kilometre-scale scalloped depressions (e.g., Figure 4) in Utopia and Acidalia Planitiae (Costard & Kargel, 1995). This suggested that massive ice existed in the shallow subsurface.

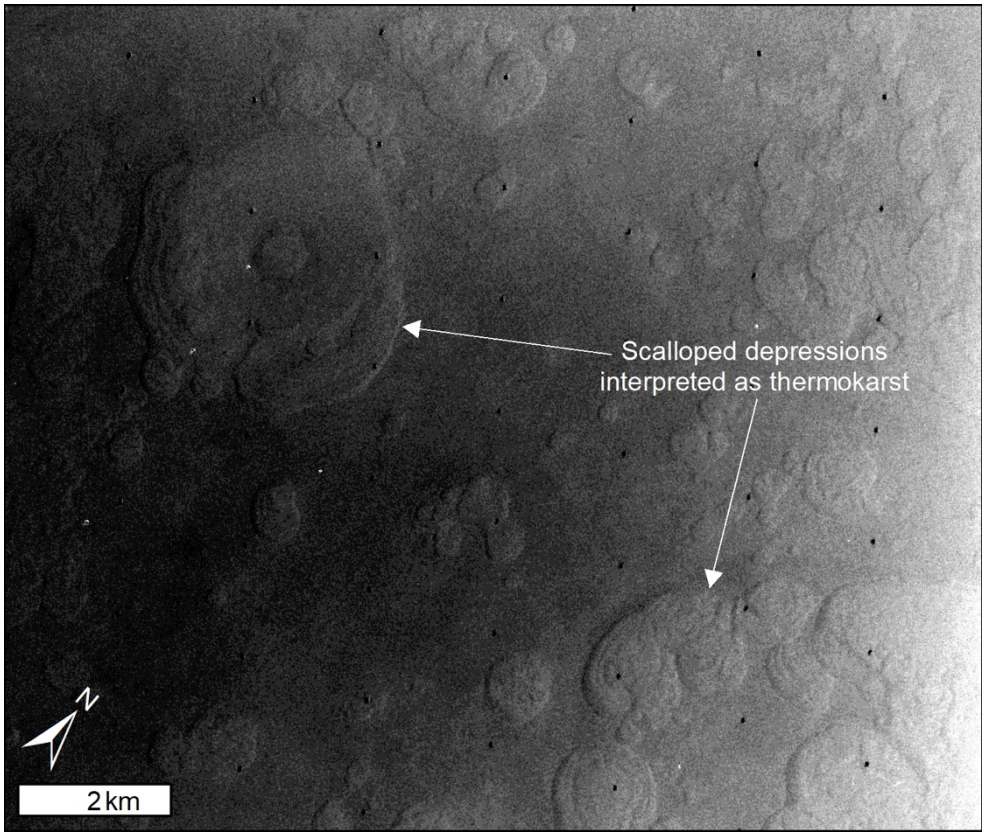

Figure 4: Scalloped Depressions in Utopia Planitia. *These features (located at ~45.5°N) were interpreted by Costard and Kargel* (1995) *as thermokarst terrain formed by loss of excess ice in the subsurface. Viking orbiter image 466B96.*

Image credit: F. Butcher, with data from NASA/JPL.

Polygonal Patterned Ground

The NASA Viking 2 lander, which touched down in Utopia Planitia (~48°N) in 1976 (Figure 5), was the first lander to operate successfully within the zone of predicted subsurface ice stability. The earlier Soviet Mars 3 lander failed seconds after landing in the mid latitudes (45°S) in 1971. The Viking 2 lander imaged networks of trough-bounded polygonal landforms (<10 m wide; Figure 5) on the surface, which were interpreted as either cracks formed by the desiccation of formerly water-saturated materials, or thermal contraction within frozen ground (Mutch et al., 1977). Excavations to depths of ~15 cm by the lander did not reach the predicted

depth to the perennial ice table (~24cm; Mellon et al., 2004; Byrne et al., 2009), and indeed no perennial ice was found.

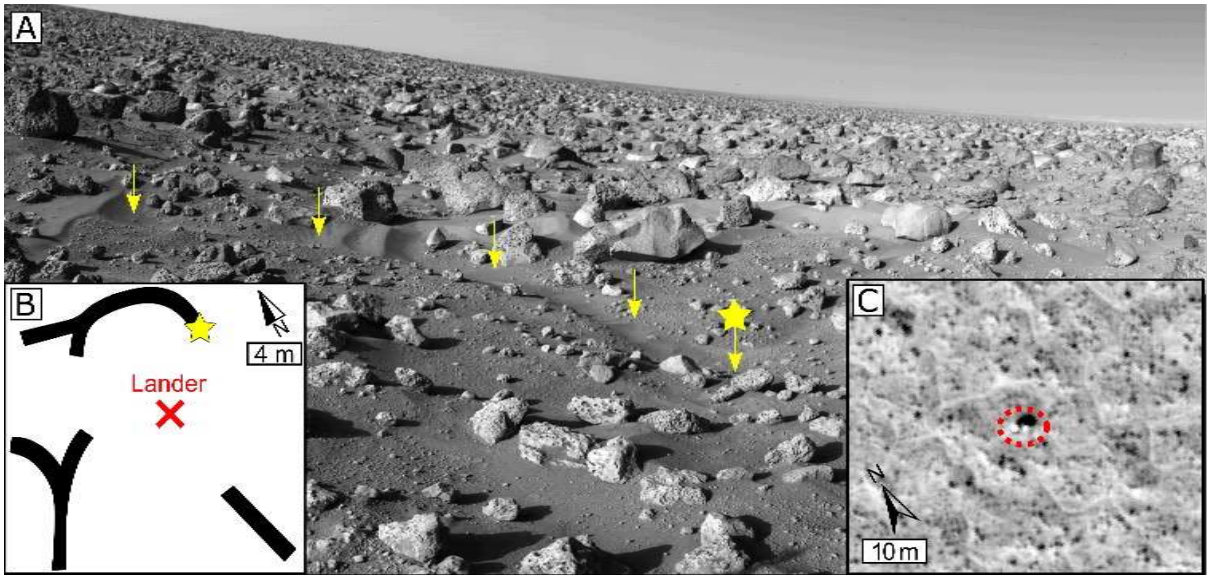

Figure 5: Polygonal trough networks observed by the Viking 2 lander. *(A) Lander photomosaic of a trough (yellow arrows). (B) Schematic map of troughs observed around the lander. Yellow star approximates the location of the star in panel A. (C) High Resolution Imaging Science Experiment (HiRISE) image of the Viking 2 lander (red dotted circle) taken in 2006, showing traces of polygonal landforms observed from orbit at 25 cm/pixel resolution.*

Image Credit: (A) F. Butcher, with data from NASA/JPL/University of Arizona. (B) Redrawn by F. Butcher from Mutch et al. (1977)*. (C) F. Butcher, with data from NASA/JPL/University of Arizona.*

Numerous large-scale polygonal (50 m–10 km wide) landforms were also identified from Viking orbiter images (e.g., Carr & Schaber, 1977; Lucchitta, 1981). However, it was recognised that their large scales (up to two orders of magnitude larger than thermal contraction polygons formed in ice-rich terrains on Earth) called into question whether they could be attributed to the presence of ice (Carr & Schaber, 1977; Pechmann, 1980; Seibert & Kargel, 2001).

New Insights from Mars Global Surveyor

The arrival of Mars Global Surveyor (MGS) in Mars' orbit in 1997 drove significant leaps in our understanding of Mars' surface and its topography. The Mars Orbiter Camera (MOC) instrument (Malin & Edgett, 2001) provided high-resolution (~2–12 m/pixel) images of the surface (albeit with limited coverage), revealing a suite of small-scale landforms (Figure 6) which provided strong support for the presence of near-surface ice in Mars' mid-to-high latitudes (e.g., Mustard et al., 2001; Seibert & Kargel, 2001; Milliken et al., 2003; Mangold et al., 2004). In addition, the Mars Orbiter Laser Altimeter (MOLA) instrument (Smith et al., 2001) provided the first high-precision global view of Mars' topography.

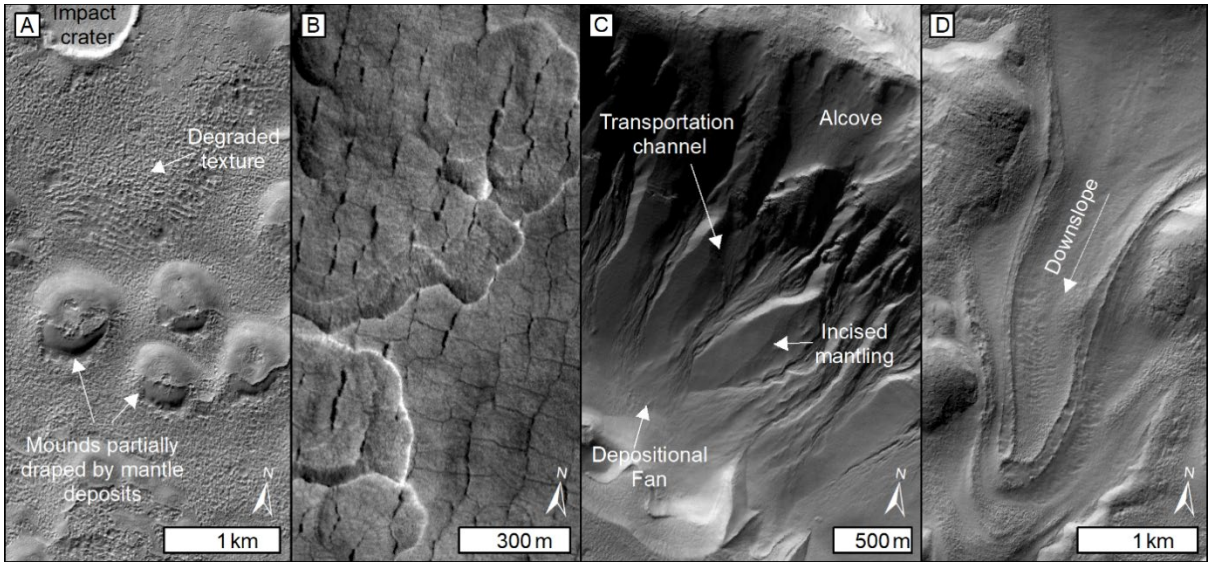

Figure 6: Small-scale landforms identified in MOC images and interpreted as being related to the presence of ice*. Illumination from left in all images. (A) Pitted and degraded mantling deposits which drape circular mounds at ~43.3°S. MOC image FHA01450. (B) Small-scale polygonal landforms on scalloped depressions interpreted as thermokarst in Utopia Planitia (~45°N). MOC image M0305694. (C) Gullies incising smooth mantling deposits on a crater wall at ~43°S. MOC image M1900651. (D) Viscous flow feature extending down a crater wall at ~38°S. MOC image M1800897.*

Image credit: F. Butcher, with data from NASA/JPL/Malin Space Science Systems. MOC images from M. C. Malin, K. S. Edgett, S. D. Davis, M. A. Caplinger, E. Jensen, K. D. Supulver, J. Sandoval, L. Posiolova, and R. Zimdar, (A) FHA01450, (B) M0305694, (C) M1900651, and (D) M1800897, Malin Space Science Systems Mars Orbiter Camera Image Gallery (http://www.msss.com/moc_gallery/), Release dates: (A) and (B) 22 May 2000, (C) 8 October 2001, (D) 4 April 2001.

Mantling Deposits and Terrain Softening

Using MOC images, Mustard et al. (2001) described a decametre-thick mantle of young material, which draped and muted underlying topography and exhibited evidence of an ice-rich composition and latitude-dependent (interpreted as climate-controlled) degradation at latitudes between 25–60° (Figure 6A). This was broadly consistent with the distribution of mantling deposits identified in earlier Mariner and Viking images (Soderblom et al., 1973; Carr & Schaber, 1977; Squyres & Carr, 1986). Analyses of MOLA topography confirmed the 'terrain softening' effect of the mantling unit (Kreslavsky & Head, 2000) that was proposed by Squyres and Carr (1986). Mustard et al. (2001) initially suggested that the mantling deposit comprised young deposits of airfall dust that was subsequently cemented by ground ice emplaced by vapour diffusion. Head et al. (2003) later argued that the combined results of the Mars Global Surveyor and Mars Odyssey missions (see 'Into the 21st Century') supported formation of the mantling deposits by cyclical deposition of excess ice via airfall during periods of high planetary obliquity within the last 2 Myr.

Polygonal Patterned Ground, Scalloped Depressions, and Gullies

MOC images also revealed small-scale (10s metres wide) polygonal terrain (Figure 6B) similar to the trough-bounded polygons previously imaged by the Viking 2 lander (Figure 5). The polygons were interpreted as having formed by thermal contraction of ice-rich ground (Seibert & Kargel, 2001; Mangold et al., 2004). Seibert and Kargel (2001) highlighted a high

concentration of small-scale polygons in Utopia Planitia, including within the scalloped depressions (Figure 6B) interpreted as thermokarst terrains from earlier Viking orbiter images (Figure 4; Costard & Kargel, 1995). This added support for the involvement of ground ice in the formation of both landforms. A global survey of MOC images by Mangold et al. (2004) demonstrated a latitudinal control on the distribution of polygonal terrains, which occurred at latitudes poleward of 55°N/S. The involvement of liquid water in the formation of polygonal terrains on Mars became a topic of prolonged discussion (see e.g., Levy, Marchant, et al., 2010). The existence of ice-wedge polygons (which form by the migration of meltwater to polygon margins) has been proposed in some locations, including in early analyses of the Viking 2 landing site (Mutch et al., 1977), but more extensive subsequent investigations suggest the infilling of polygon margins by sand wedges was probably the dominant process over large regions (e.g., Levy, Head, et al., 2010).

Another intriguing type of landform revealed in MOC images was young (less than a few million years old), kilometre-scale gullies on steep slopes such as crater walls (Figure 6C; Malin & Edgett, 2000). Gullies comprise an erosional alcove, a transportation channel, and a depositional fan. Malin and Edgett (2000) initially proposed that gullies on Mars were carved by liquid water discharged from perched groundwater aquifers. However, subsequent MOC-era studies (Christensen, 2003; Milliken et al., 2003) noted that they are commonly associated with (and often carve into) ice-rich mantling materials similar to those identified by Mustard et al. (2001). This led to the inference that geologically-recent melting of ice within the mantling deposits supplied liquid water for gully formation (Christensen, 2003; Milliken et al., 2003). The discovery of gullies sparked a decades-long debate over the involvement of water in their formation. Could gully-forming flows of liquid water exist on recent Mars (e.g., Knauth, 2000; Hecht, 2002), or could gullies be explained by other mechanisms relating to carbon dioxide processes (e.g., mass wasting triggered by carbon dioxide phase changes which

do not occur naturally on Earth; e.g., Musselwhite et al., 2001; Hoffman, 2002)? If water was required, what were its potential sources (e.g., Malin & Edgett, 2000; Costard et al., 2002; Christensen, 2003; Milliken et al., 2003)? This debate has not been completely resolved. Ongoing mass movement activity has been observed within gullies (e.g., Reiss and Jaumann, 2003; Malin et al., 2006), leading to suggestions that liquid water is not essential, at least for their contemporary evolution (e.g., Diniega et al., 2010; Dundas et al., 2010). It is possible that multiple mechanisms (including those involving water ice and carbon dioxide ice) have influenced gully evolution as climate conditions have varied over time. The reader is directed to Conway et al. (2018) for a comprehensive review.

Ice-Rich Viscous Flow Features

In a global survey of MOC images, Milliken et al. (2003) identified kilometre-scale landforms termed 'viscous flow features' (Figure 6D) within ice-rich materials similar to those described by Mustard et al. (2001). These features, which host surface lineations suggestive of flow, are bounded at their downslope ends by arcuate ridges of deformed material, occur exclusively within Mars' mid latitudes (between 30–60°N/S), and are most common at ~40°N/S. Milliken et al. (2003) suggested that the latitude-dependence of these flows resulted from temperature-dependence of ice-assisted creep, which prevented similar flow of ice-rich materials at colder, higher latitudes (Milliken et al., 2003). Independent analyses of topographic concavity by Kreslavsky and Head (2002) identified a distinctive band of concave topography in the ~30–60°N/S latitude band, which they interpreted as having been generated by the flow of ice-rich materials.

Milliken at al. (2003) suggested that the small viscous flow features could be small-scale end-members of the larger lineated valley fills, lobate debris aprons, and concentric crater fills identified in earlier Mariner and Viking orbiter images (Figure 3). They argued that the small-scale viscous flows might have originated as ice-rich deposits which accumulated by the

cyclical deposition of ice and dust layers by airfall (i.e. as dusty snow deposits), during recent episodes of high planetary obliquity.

Several workers also returned to analyses of the larger scale lineated valley fills, concentric crater fills and lobate debris aprons (Figure 3) using Mars Global Surveyor data. However, these studies seemed unable to resolve the debate over the origins of these features and the original ice content required to form them. While Colaprete and Jakosky (1998) argued that they originated with high ice contents (up to 80% by volume), most studies supported a debris-rich composition derived from mass wasting processes (e.g., Mangold & Allemand, 2001; Mest & Crown, 2001; Mangold et al., 2002; Pierce & Crown, 2003), perhaps with ice contents as low as ~30% by volume (Mangold et al., 2002).

Into the 21st Century

The arrivals of NASA's Mars Odyssey (orbital entry: 2001), ESA's Mars Express (orbital entry: 2003), NASA's Mars Reconnaissance Orbiter (orbital entry: 2006), and NASA's Phoenix lander (which touched down at 68°N in 2008) drove significant advances in our understanding of water ice in Mars' mid latitudes.

Improvements in the resolution and coverage of orbital imaging of Mars' surface (e.g., near global 6 m/pixel coverage from the Context Camera (CTX; Malin et al., 2007), and 25 cm/pixel coverage of smaller areas with the High Resolution Imaging Science Experiment (HiRISE; McEwen et al., 2007) instruments, both onboard NASA's Mars Reconnaissance Orbiter) have enabled more detailed estimations of the ages mid-latitude ice deposits. The ages of planetary surfaces can be modelled based on statistics of the number and size of impact craters within a given area (e.g., Hartmann & Neukum, 2001; Ivanov, 2001; Hartmann, 2005). Dating of young ice deposits on Mars is affected by significant uncertainties (e.g., Hartmann, 2005; Michael et

al., 2012; Warner et al., 2015), but it is possible to obtain first-order estimates of their relative ages and minimum absolute ages.

Subsurface Ice at Depths Shallower than 1 m

The distribution of shallow (<1 m depth) ice identified on Mars is in general agreement with early theoretical predictions (e.g., Leighton & Murray, 1966). The Gamma Ray Spectrometer (GRS; Boynton et al., 2004) suite on board NASA's Mars Odyssey and the Fine Resolution Neutron Detector (FREND; Mitrofanov et al., 2018) on ESA-Roscosmos ExoMars Trace Gas Orbiter (orbital entry: 2016) detected neutrons released from hydrogen atoms in Mars' subsurface following excitement by cosmic rays. These detections were used to generate maps (with spatial resolutions of several tens to hundreds of kilometres) of water-equivalent hydrogen (ice) content in the upper 1 m of Mars' subsurface (e.g., Figure 7). The maps suggest that excess ice (>50% up to 100% by volume) is present within 1 m of the surface poleward of ~50°N/S, extending down to ~45° latitude in the Arcadia Planitia and Promethei Terra regions of the northern and southern hemispheres, respectively (Boynton et al., 2002; Feldman et al., 2004; Kuzmin et al., 2004; Mitrofanov et al., 2004; Feldman et al., 2011; Pathare et al., 2018; Malakhov et al., 2020). The distribution of polygonal landforms (e.g., Figure 5 and 6B), which are interpreted as thermal contraction polygons formed in ice-rich ground, agrees well with the latitudinal boundary of shallow ice detections (Mangold et al., 2004).

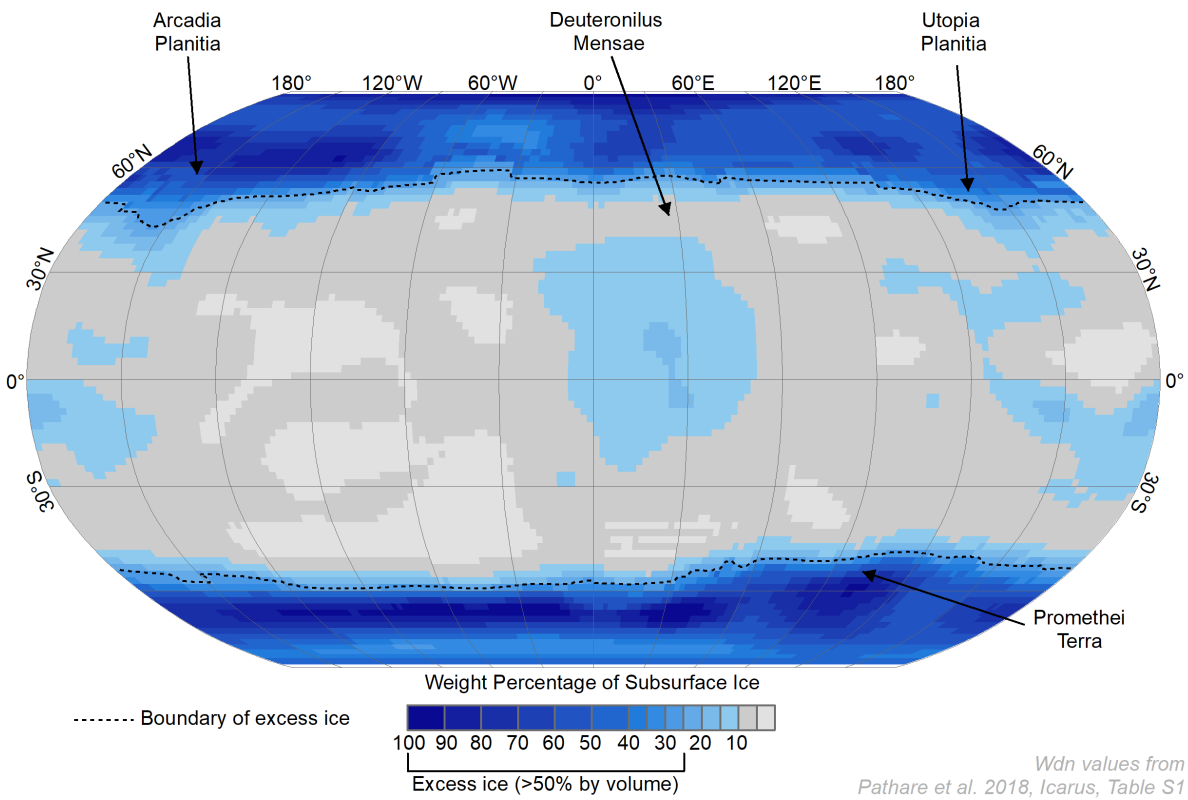

Figure 7: Map of Subsurface Ice at Depths <1 m from Mars Odyssey Neutron Spectrometer. *Colours represent the weight percentage of subsurface ice, where values >25 likely represent excess ice exceeding the pore space of the regolith (the boundary of which is indicated by the dotted line). Plotted with data from Deconvolved {N=16} Solution Wdn values in Table S1 of Pathare et al. 2018.*

Image Credit: F. Butcher, with data from Pathare et al. (2018).

Independent shallow ice maps generated from thermal analyses using various orbital spectrometer instruments broadly agree with the GRS and FREND maps (Bandfield & Feldman, 2008; Bandfield, 2007; Piqueux et al., 2019). In a higher (10s of kilometres) resolution map generated from the Mars Climate Sounder spectrometer (McCleese et al., 2007) onboard Mars Reconnaissance Orbiter, Piqueux et al. (2019) noted an additional detection of shallow ice extending down to a latitude of ~35°N in the Deuteronilus-Protonilus Mensae region which did not appear in earlier, lower-resolution maps. The presence of discontinuous

near-surface ice at latitudes as low as ~24°N/S was predicted by Aharonson and Schorghofer (2006), whose thermal modelling suggested that metre-scale topographic roughness could permit the stability of near-surface ice deep into the mid latitudes. Spectral observations of seasonal carbon dioxide frost deposition in the southern hemisphere also support the presence of subsurface water ice towards the low mid-latitudes (Vincendon et al., 2010). Vincendon et al. (2010) observed that seasonal CO_2 frosts do not extend as far towards the equator as might be expected in the absence of near-surface water ice.

NASA's Phoenix lander, which touched down at ~68°N in 2008, provided the first direct imaging of subsurface ice beyond Mars' polar regions (Figure 8; Mellon et al., 2009; Smith et al., 2009). Phoenix excavated ground ice (Figure 8A) in terrain hosting thermal contraction polygons (Figure 8B), at an average depth of ~4.6 cm (Mellon et al., 2009; Smith et al., 2009). While 90% of the ice excavated by the lander was pore-filling ice, ~10% was present in segregated lenses of excess ice which could not be explained by vapour diffusion from the atmosphere alone (Mellon et al., 2009). A 10% excess ice composition was, however, lower than the predominantly excess ice composition predicted in the Mars Odyssey GRS maps (Figure 7).

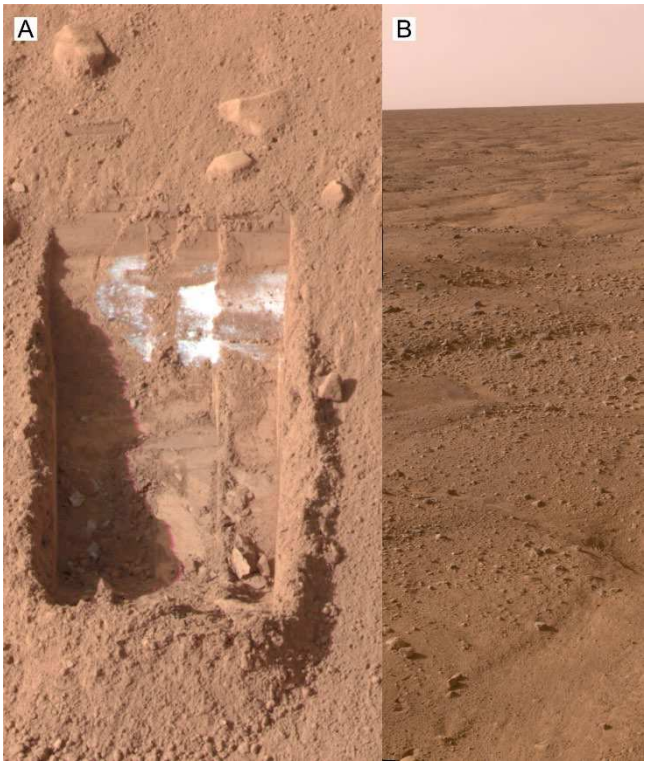

Figure 8: Evidence for Ground Ice at the Phoenix Landing Site at ~68°N. *(A) A trench (~15 cm wide) excavated by the Phoenix Lander revealing excess ice centimetres beneath the surface. (B) A view across the landscape from the Phoenix landing site, showing extensive polygonal trough networks interpreted as thermal contraction cracks.*

Image credit: NASA/JPL-Caltech/University of Arizona/Texas A&M University/F. Butcher

Pathare et al. (2018) reanalysed the Mars Odyssey GRS data, this time modelling ice contents based on a 3-layer model of the upper 1 m of the subsurface (in contrast to simpler 2-layer models used to generate earlier maps). Pathare et al. (2018) suggested that the orbital detections for the Phoenix landing site could be explained by the presence of a thin desiccated surface layer (confirmed by the lander) which overlies a layer of predominantly pore-filling ice (also confirmed by the lander), which overlies a layer of pure excess ice at a depth of 19.2 cm. The depth to the pure ice layer in the updated GRS analyses is 0.9 cm deeper than the maximum depth excavated by the Phoenix lander (Mellon et al., 2009), and could explain why the it encountered predominantly pore-filling ice (Pathare et al., 2018).

High-resolution (25 cm/pixel) orbital images from the HiRISE camera provide independent confirmation that excess ice is indeed abundant in the upper metre or so of the subsurface in Mars' mid latitudes (Byrne et al., 2009; Dundas et al., 2014, 2021). Small (typically 1–25 m diameter) fresh impact craters (which penetrate up to ~2 m into the subsurface, depending on the size of the impact) exhumed bright ice deposits (Figure 9) in regions >~40°N/S (Byrne et al., 2009; Dundas et al., 2014, 2021). Repeat imaging demonstrated that, as expected, the ice sublimated away within a few months (Byrne et al., 2009).

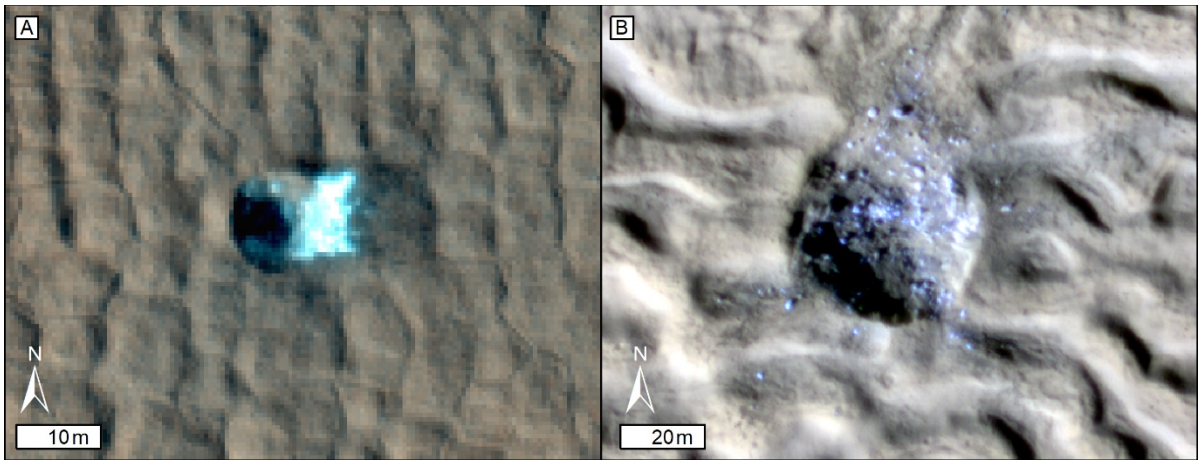

Figure 9: Excess ice exposed by small, fresh impacts in Mars' mid latitudes. *Illumination from left in both panels (A) A small, fresh impact crater identified by Byrne et al.* (2009)*, which has exhumed bright ice in terrain hosting thermal contraction polygons at ~46°N. HiRISE false colour image ESP_011494_2265. (B) A small, fresh, ice-exposing impact crater identified by Dundas et al.* (2021)*. The impact crater is on the surface of a lineated valley fill-type viscous flow feature at ~41°N. The impact has exhumed large blocks of high purity ice, which could be derived from buried glacial ice. HiRISE false colour image ESP_046707_2220.*

Image Credit: NASA/JPL/University of Arizona/F. Butcher

Subsurface Ice beyond ~1 m Depth

There is also abundant evidence for the presence of subsurface ice beyond ~1 m depth in Mars' mid latitudes. Identified deposits are predominantly within the upper tens to hundred metres of the subsurface. Deeper ice deposits might be present (derived, for example, from burial of surface deposits or freezing of deep groundwater), but signatures of such deep deposits remain elusive to (or out of reach of) existing techniques (e.g., Clifford et al., 2010).

Global reflectivity maps from the Mars Advanced Sounder for Ionosphere and Subsurface Sounding (MARSIS; Picardi et al., 2004) on board ESA's Mars Express, which characterise the dielectric properties of the upper tens of metres of Mars subsurface, suggest that this layer hosts 50–100% water ice by volume at latitudes >40°N/S (Mouginot et al., 2010).

Subsurface returns detected by the Mars Reconnaissance Orbiter Shallow Radar (SHARAD; Seu et al., 2007) instrument have also been used to infer decametre-thick buried layers of subsurface ice in the plains of Arcadia Planitia (Bramson et al., 2015) and Utopia Planitia (Stuurman et al., 2016). However, independent analyses of the strengths of SHARAD radar echo signals with different frequencies have also been used to suggest that high-ice-purity materials might be restricted to a relatively shallow layer in these regions (Campbell & Morgan, 2018; see also Morgan et al., 2021). Despite this, the radar detections do coincide with numerous observations suggestive of the presence of a significant volume of subsurface ice. The radar detections in Utopia Planitia coincide with scalloped depressions such as those identified in Viking and MOC images (Figure 4 and 6B; Costard & Kargel, 1995; Seibert & Kargel, 2001). The radar detections in Arcadia Planitia coincide with a regional maxima in Mars Odyssey near-surface (<1 m) ice detections (e.g., Pathare et al., 2018), and unusual crater morphologies including 'expanded' impact craters interpreted to have been modified by sublimation thermokarst processes (Viola et al., 2015), and craters with terraced interior morphologies interpreted as having formed by the penetration of an impactor into a subsurface

layer hosting excess ice (Bramson et al., 2015; Martellato et al., 2020). Age determinations from impact crater counting suggest that subsurface ice in Arcadia Planitia could be tens of millions of years old (Viola et al., 2015).

Scalloped depressions and expanded impact craters have also been identified in other mid-latitude regions, including in the southern hemisphere (e.g., Morgenstern et al., 2007; Lefort et al., 2009, 2010; Zanetti et al., 2010; Viola & McEwen, 2018). They are most widely attributed to the decay of excess subsurface ice by insolation-driven sublimation (e.g., Morgenstern et al., 2007; Lefort et al., 2009; Séjourné et al., 2011; Dundas et al., 2015), although melting of ground ice has also been proposed as a formation mechanism (e.g., Soare et al., 2008).

Latitude-Dependent Mantle

The latitude-dependent mantle (LDM) is a young ice-rich deposit in Mars' mid-to-high latitudes (Figure 10). It drapes terrain (Figure 10A) with near-continuous coverage at latitudes >55°N, and becomes thinner, more degraded and discontinuous towards the mid-latitude boundaries of its distribution (~30°N and 25°S; Mustard et al., 2001; Head et al., 2003). Here, it is preferentially preserved on cooler pole-facing slopes and crater walls (Christensen, 2003; Schorghofer & Aharonson, 2005; Conway & Mangold, 2013). Kreslavsky and Head (2002) estimated that the LDM covers ~23% of Mars' surface. Deposit thicknesses measured using HiRISE images (and ~1 m/pixel resolution 3D elevation models generated from them) of natural incisions through the LDM (Figure 10B–C) demonstrate that it reaches tens of metres, up to ~100 m in thickness (e.g., Conway & Balme, 2014; Dundas et al., 2018, 2021).

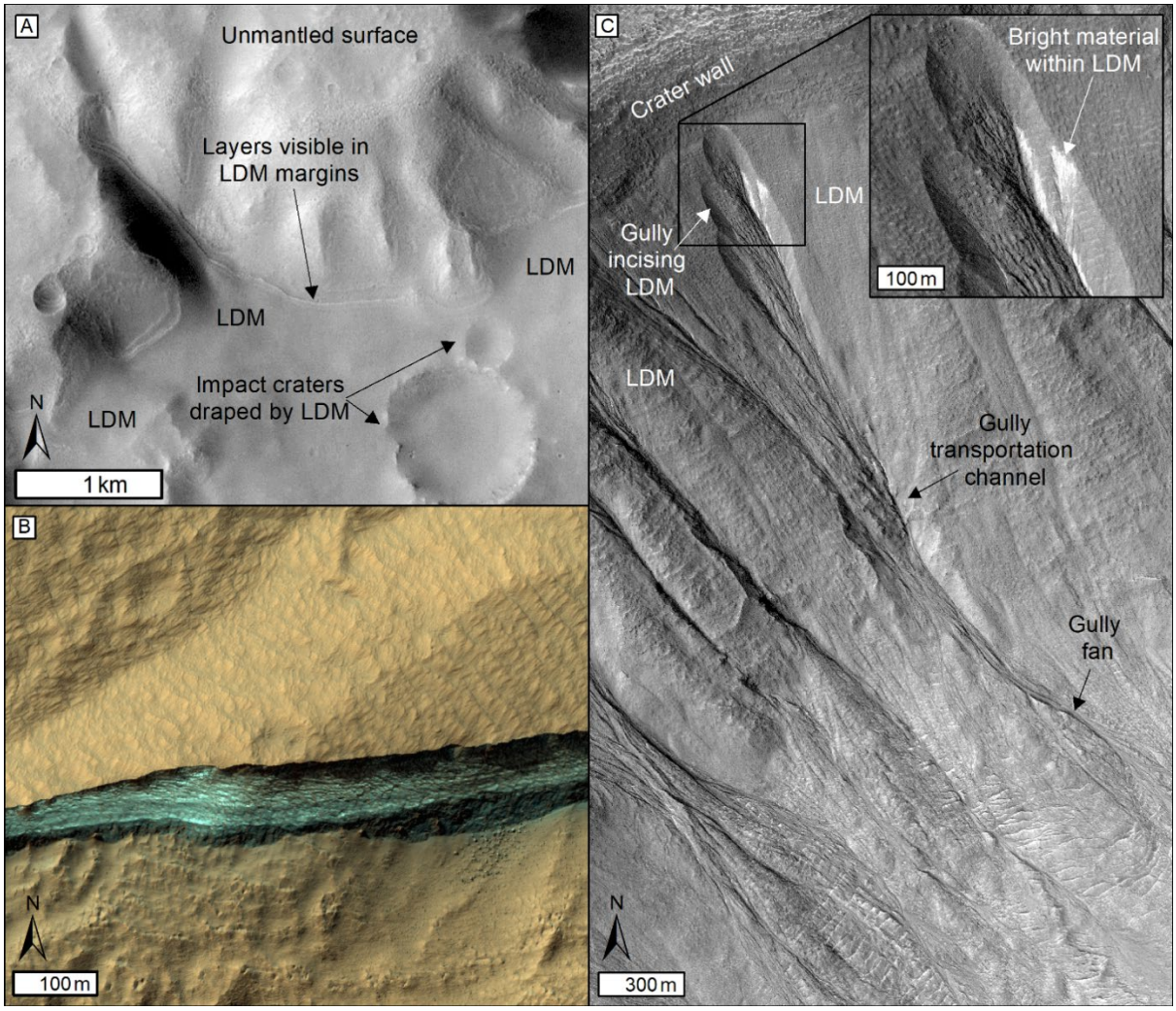

Figure 10: The latitude-dependent mantle (LDM). *Illumination from left in all panels. (A) Layers identified by Head et al.* (2003) *in the margins of discontinuous LDM deposits at 35.1°S, which drape topography including impact craters. CTX image P08_003992_1469_XN_33S174W. (B) False colour HiRISE image looking into a hundred-metre-high scarp identified by Dundas et al.* (2018) *at 58.1°S. The scarp exposes thick, bright, high-purity ice deposits in the LDM. HiRISE image ESP_040772_1215. (C) A gully incising into LDM at 32.9°S. The inset shows bright materials within the gully alcove, which are interpreted by Khuller and Christensen* (2021) *as exposed water ice. HiRISE image ESP_013067_1470.*

Image Credit: F. Butcher, with data from: (A) NASA/JPL-Caltech/Malin Space Science Systems, (B) and (C) NASA/JPL/University of Arizona

Ice Content of the Latitude-Dependent Mantle

As suggested by Milliken et al. (2003), there is evidence that the LDM hosts a substantial volume fraction of water ice in excess of that which can be expected from vapour diffusion from the atmosphere alone, suggesting instead that it was deposited via airfall.

The surface of the LDM hosts extensive fields of small-scale polygons similar to those observed at the Viking 2 and Phoenix landing sites (Figure 5 and 8; Mutch et al., 1977;. Mellon et al., 2009), which are widely interpreted as thermal contraction cracks formed in buried ice or ice-cemented materials (e.g., Mutch et al., 1977; Seibert & Kargel, 2001; Mellon et al., 2009; Smith et al., 2009; Levy, Head, Marchant, et al., 2009; Levy, Marchant, et al., 2010).

Striking (albeit spatially-restricted) visual evidence for a bulk ice composition comes from exposed cliffs with heights of up to ~100 m within mid-latitude mantling deposits (Figure 10B), which are actively retreating due to ice sublimation from the cliff faces (Dundas et al., 2018, 2021; Harish et al., 2020). In some locations, the cliffs expose thick, bright materials that are spectrally consistent with high-purity ice (Dundas et al., 2018, 2021). The locations of ice-exposing scarps are, however, concentrated around the southern rim of the Hellas basin and within Arcadia Planitia, and may not be typical of wider LDM materials (Dundas et al., 2021). Smaller exposures of bright materials interpreted as dusty water ice have also been identified in the alcoves of gullies (Figure 10C) incised into polygonised LDM deposits at latitudes down to ~33°S (Khuller & Christensen, 2021).

The LDM becomes increasingly dissected, hummocky and pitted towards the mid-latitude boundary of its distribution (Figure 6A), which likely reflect the degradation of its ice content by sublimation towards warmer latitudes (e.g., Mustard et al., 2001; Head et al., 2003).

Estimates of the ice content of the LDM suggest that it hosts the equivalent of a global layer of water ~2.5 m deep (Head et al., 2003; Levy, Marchant, et al., 2010).

Age of the Latitude-Dependent Mantle

Modelled ages derived from impact crater size-frequency statistics suggest that most of the latitude-dependent mantle was emplaced since 2 Myr ago (Kostama et al., 2006; Levy, Head, & Marchant, 2009a; Schon et al., 2012). Layering observed in the margins of LDM deposits (Figure 10A) suggests that it was emplaced in multiple episodes (Head et al., 2003; Schon et al., 2009). The modelled ages become younger towards higher latitudes, being 1–2 Myr at ~30–50°N/S, hundreds of thousands of years in the mid-to-high latitudes, and <100 kyr approaching the polar regions (Kostama et al., 2006; Levy, Head, & Marchant, 2009a; Schon et al., 2012).

Ice-Rich Viscous Flow Features

The term viscous flow feature is used to refer to both the large lobate debris aprons (Figure 11A), lineated valley fills (Figure 11A–B), and concentric crater fills (Figure 11C) first identified in Mariner and Viking orbiter images (Figure 3; Sharp, 1973; Squyres, 1978, 1979), and the smaller flow features (Figure 6) identified in MOC images by Milliken et al. (2003). The small-scale viscous flow features (Figure 11D) were termed ‘glacier-like flows’ by Arfstrom and Hartmann (2005), and later renamed as ‘glacier-like forms’ by Hubbard et al. (2011). In many locations these features merge into one-another in various configurations (Figure 11A), forming integrated, composite flows (Head et al., 2006). Towards the higher mid latitudes, their surfaces are superposed by younger latitude-dependent mantle deposits (e.g., Mangold, 2003; Levy, Head, & Marchant, 2009b; Baker & Carter, 2019a).

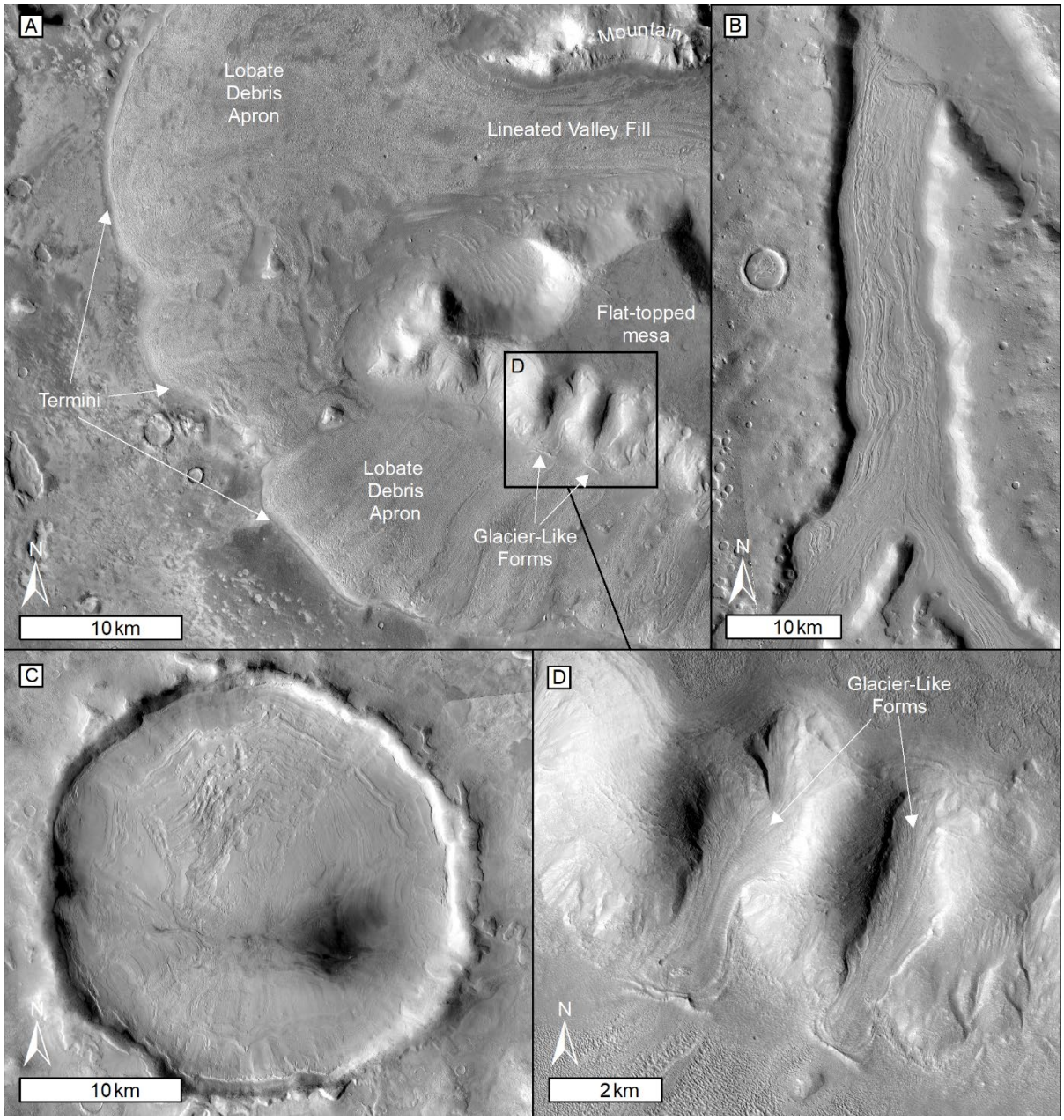

Figure 11: Context Camera image mosaics of Viscous flow features in and around Protonilus Mensae. *(A) A complex of lobate debris aprons (the same features shown in earlier Viking orbiter images in Figure 3B) extending from a flat-topped mesa. The lobate debris apron towards the top of the image is fed from the east by a lineated valley fill. The southern slopes of the mesa host kilometre-scale alcoves containing glacier-like forms (black box shows extent of panel D). (B) Lineated valley fill. (C) Concentric crater fill. (D) Two glacier-like forms.*

Image Credit: F. Butcher, with data from NASA/JPL-Caltech/Malin Space Science Systems

Glacier-like forms (Figure 11D) are the smallest end-member of VFFs. They are typically located in high-relief areas, originating from kilometre-scale bedrock alcoves, and extending up to ~10 km downslope before terminating at raised arcuate ridges which bound their termini (Souness et al., 2012). The arcuate ridges are morphologically similar to terminal moraine ridges on Earth, which comprise lithic material transported by the flow of glacial ice (Arfstrom & Hartmann, 2005; Milliken et al., 2003; Souness et al., 2012).

Lineated valley fills (Figure 11B) are larger valley-confined features with lengths of up to hundreds of kilometres and widths of tens of kilometres. Their surfaces host extensive valley-parallel lineations and features similar to medial moraines on Earth (which transport bands of debris down-flow in valley-parallel ridges). Where lineated valley fills reach the outlets of their host valleys, they commonly transition into lobate debris apron-type viscous flow features (Figure 11A).

Lobate debris aprons (Figure 11A) have lengths of tens of kilometres and are often wider than they are long. They are typically hundreds of metres thick, and are similar to piedmont glaciers on Earth, which spread out over flat plains due to a lack of topographic confinement. Lobate debris aprons often originate at steep headwalls and extend over flat plains, commonly forming radial complexes around isolated hills and mesas.

Concentric crater fills (Figure 11C) cover the floors of mid-latitude impact craters (e.g., Levy, Head, et al., 2010). They typically have concentric ridges and troughs on their surfaces. Where they attain sufficient thickness to fill the depth of the host crater, they often flow out via topographic lows in the host crater rim, and can merge with other viscous flow feature subtypes. In the lower mid latitudes, viscous flow features within impact craters often do not fill the entire floor of their host craters, and instead are more similar to lobate debris aprons extending part

way across crater floors (often from their pole-facing walls; e.g., Dickson et al., 2012; Levy, Head, et al., 2010).

Global-scale and regional-scale mapping efforts, have revealed the detailed distributions of each of these features (Figure 12; e.g., Souness et al., 2012; Dickson et al., 2012; Levy et al., 2014; Berman et al., 2021). Viscous flow features are concentrated in the mid-latitude regions, between ~25–60°N/S. Concentric crater fills are almost ubiquitous within these regions, but the other three subtypes are concentrated in regions such as Deuteronilus Mensae, Phlegra Montes, Tempe Terra, Promethei Terra, Charitum Montes, and Nereidum Montes (Figure 12).

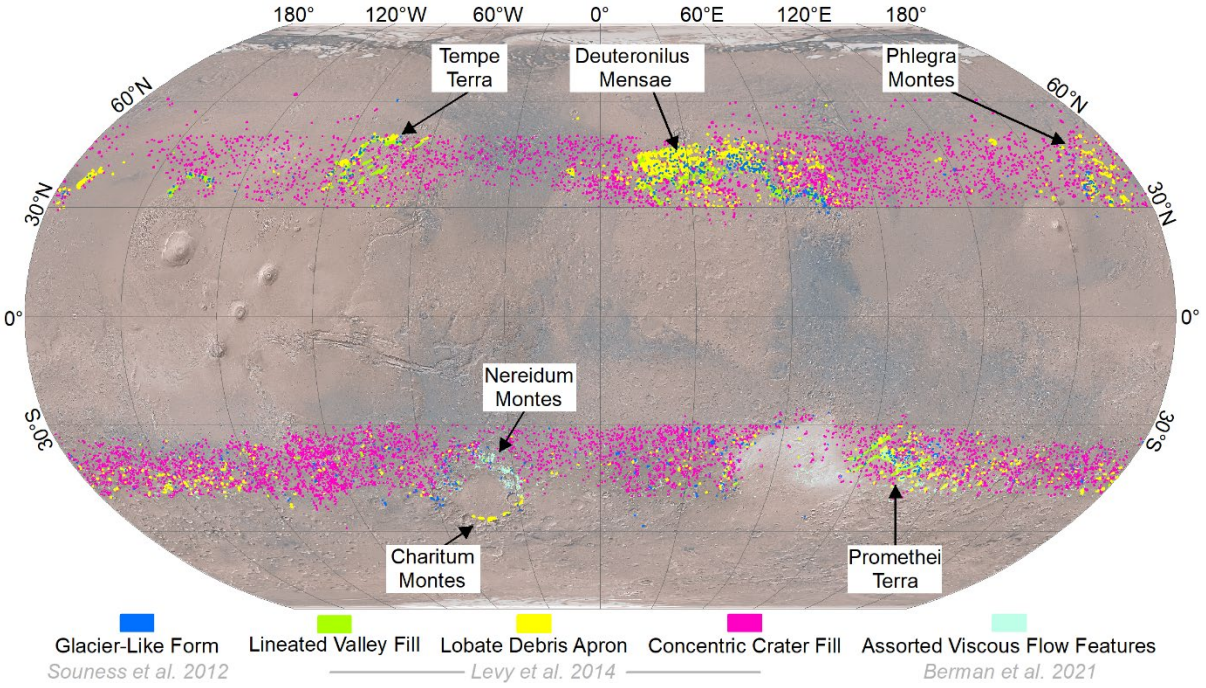

Figure 12: The distribution of mid-latitude viscous flow features on Mars. *Glacier-like forms were mapped by Souness et al.* (2012)*, and larger lineated valley fills, lobate debris aprons, and concentric crater fills were mapped by Levy et al.* (2014)*. Additional, assorted Viscous Flow Features were mapped by Berman et al.* (2021) *in Nereidum Montes. The basemap is MOLA shaded relief overlain by a Viking Orbiter Colourised Mosaic.*

Image credit: F. Butcher, with data from Souness et al. 2012, Levy et al. 2014, Berman et al. 2021,NASA, and USGS.

Ice Content of Viscous Flow Features

Images returned from the High Resolution Stereo Camera (HRSC; Neukum et al., 2004; Jaumann et al., 2007) on board ESA's Mars Express, which provided more extensive coverage than earlier MOC images (albeit at lower resolutions of >10 m/pixel), prompted Head et al. (2005) to challenge earlier hypotheses that viscous flow features were debris rich. They argued that such extensive flows could not be accounted for by mass-wasting from adjacent hillslopes as the dominant source of material (Head et al., 2003). Further analyses of the features have revealed surface structures that are strikingly similar to flow-related structures on glaciers on Earth (including flow deformation patterns, crevasses and moraine ridges comprising debris emplaced by the flow of glacial ice e.g.; Head et al., 2006, 2010; Hubbard et al., 2011).

Ground-penetrating radar observations from SHARAD provide strong support for the debris-covered glacier model. Subsurface reflectors interpreted as the beds of lobate debris apron-type features have been used to infer dielectric properties consistent with bulk water ice compositions in several locations (Holt et al., 2008; Plaut et al., 2009; Petersen et al., 2018; Gallagher et al., 2021). Instrument constraints mean that SHARAD has not been able to provide insight on the subsurface properties of smaller (kilometre-scale) or crater/valley-confined viscous flow features. However, the morphological and distributional similarities between viscous flow feature subtypes (e.g., Souness et al., 2012; Levy et al., 2014), and the fact that they commonly flow into one-another (Figure 11A; e.g., Head et al., 2006), suggests that they have similar origins. SHARAD has also been unable to detect the interface between the supraglacial debris cover and the underlying massive ice, leading to the inference that this interface is shallower than the minimum depth (~10–20 m) that the instrument can resolve (Holt et al., 2008; Plaut et al., 2009; Petersen et al., 2018; Gallagher et al., 2021). Blocks of

high purity ice (Figure 9B) exhumed by fresh impacts into the surfaces of lineated valley fill (Dundas et al., 2021) and lobate debris aprons (Byrne et al., 2009) could have been derived from the top of the glacial ice, at depths of ~1–2 m.

Volume estimates for viscous flow features on Mars suggest that, in the present day, they could host ice in volumes equivalent to a global layer of liquid water ~2.6 m deep (Levy et al., 2014; Brough et al., 2019). However, there is evidence that viscous flow features have thinned and retreated somewhat from thicker, more extensive deposits in the past (e.g., Dickson et al., 2010; Hauber et al., 2008; Hubbard et al., 2011; Dickson et al., 2012; Souness & Hubbard, 2013; Brough et al., 2016; Hepburn et al., 2020). Some workers suggest that viscous flow features are the much-receded remnants of kilometre-thick ice sheets that formerly inundated topography before retreating into confined valleys and craters (e.g., Dickson et al., 2008, 2010; Fastook & Head, 2014; Baker & Head, 2015; Baker & Carter, 2019a). A lack of widespread, landscape-scale evidence for melting strongly suggests that the majority of ice loss has been by sublimation. However, rare landforms such as fresh, shallow valleys on and around viscous flow features (Fassett et al., 2010; Hobley et al., 2014), and candidate eskers (ridges of sediment deposited by meltwater flowing through tunnels beneath glacial ice; Gallagher & Balme, 2015; Butcher et al., 2017, 2020, 2021) have been posited as evidence for rare, localised melting in a handful of locations. The larger viscous flow features have convex topographic profiles (e.g., Pierce & Crown, 2003) suggesting that they retain substantial cores of glacial ice in the present day. Many of the smaller glacier-like forms have more concave topographic profiles and may have lost a substantial proportion of their original ice content (e.g., Milliken et al., 2003; Hubbard et al., 2011; Brough et al., 2016). Glacier-like forms may be more sensitive to climatic changes than the larger viscous flow feature subtypes due to their small initial volumes and steep topographic settings (Brough et al., 2016).

Ages of Viscous Flow Features

Stratigraphic relationships and age estimations from impact crater size-frequency statistics both demonstrate that viscous flow features are older than the latitude-dependent mantle (e.g., Levy, Head, & Marchant, 2009b; Baker & Carter, 2019a). However, modelled ages still place the formation of viscous flow features in Mars' relatively recent geologic history. Modelled ages for the lobate debris aprons, lineated valley fills and concentric crater fills range between hundreds of millions and 1 billion years (e.g., Levy et al., 2007; Levy, Head, et al., 2010; Baker & Head, 2015; Gallagher & Balme, 2015; Butcher et al., 2017; Baker & Carter, 2019b). In some locations, glacier-like forms superpose larger viscous flow features rather than merging continuously into them (Brough et al., 2015; Hepburn et al., 2020), and have correspondingly younger modelled ages (clustering around 2–20 and 45–65 Myr; Hepburn et al., 2020; see also: Arfstrom & Hartmann, 2005; Hartmann et al., 2014; Hepburn et al., 2020). This suggests that Mars has experienced multiple phases of glaciation within the last 1 billion years and that ice has been preserved through multiple cycles (e.g., Brough et al., 2015; Hepburn et al., 2020).

Emplacement of Mid-Latitude Ice Deposits

It is widely agreed that, in general, the thick subsurface ice deposits identified in Mars' mid latitudes were probably deposited by precipitation (e.g., as snow), with vapour diffusion emplacing only shallow pore-ice deposits to shallow depths (e.g., Head et al., 2003; Milliken et al., 2003; Head et al., 2005; Holt et al., 2008; Bramson et al., 2015; Dundas et al., 2021).

The dominant control on the mobilisation and redistribution of ice on Mars over time has been its axial tilt (obliquity), which has undergone much higher-magnitude variations (between 15 and 45° in the recent past; Laskar & Robutel, 1993; Touma & Wisdom, 1993; Laskar et al., 2004) than Earth (~±1.3°; Laskar et al., 1993). Mars' orbital parameters are best constrained back to 20 Myr ago (Laskar et al., 2004) and are illustrated in Figure 13.

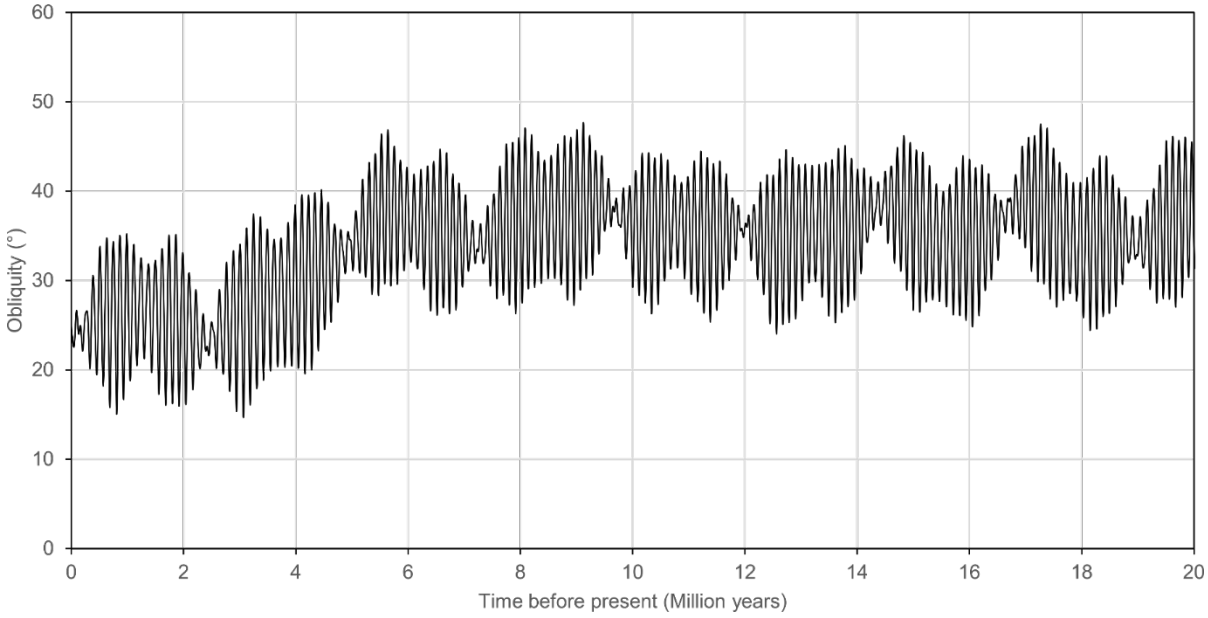

Figure 13: Variations in Mars' Obliquity back to 20 Million Years Ago.

Image Credit: Redrawn by F. Butcher from Laskar et al. 2004

General circulation models have simulated the redistribution of ice on Mars under different orbital parameters (e.g., Mischna et al., 2003; Forget et al., 2006; Levrard et al., 2007; Madeleine et al., 2009). At current obliquity, surface ice is stable in the polar regions (Levrard et al., 2007). However, it becomes destabilised under warmer temperatures at obliquities ~>30° (Levrard et al., 2007). At intermediate obliquities (~35°), ice is preferentially stable in the mid latitudes (e.g., Mischna et al., 2003; Levrard et al., 2004, 2007; Madeleine et al., 2009), and at high obliquities (~45°), it is preferentially stable in the equatorial regions (Mischna et al., 2003; Levrard et al., 2004; Forget et al., 2006). Modelling by Madeleine et al. (2009) demonstrates foci of mid-latitude ice deposition at ~35° obliquity in regions broadly coincident with observational evidence for excess subsurface ice. Modelled foci of equatorial ice deposition at 45° obliquity (Forget et al., 2006) coincide with features interpreted as relicts of past glaciers on the flanks of the large equatorial volcanoes (e.g., Head et al., 2005; Shean et al., 2005, 2007; Kadish et al., 2008).

Between ~5 and 20 Myr ago, Mars' average obliquity was ~35°, varying between ~25 and 45° in ~120 kyr cycles (Figure 13). This likely permitted the long-term accumulation of ice in Mars' mid latitudes, with periodic remobilisation to equatorial and high latitudes.

Between ~5 Myr and ~400 kyr ago, Mars' average obliquity was ~25° (Figure 13). This likely drove the long-term accumulation of Mars' present polar caps at the expense of non-polar ice reservoirs (Levrard et al., 2007). Approximately 30 cyclic excursions to intermediate obliquity punctuated this period and may have permitted short episodes of ice accumulation in the mid-to-high latitudes (e.g., Head et al., 2003; Levrard et al., 2004, 2007). The relative quiescence of Mars' obliquity, at around 25°, since ~400 kyr ago (Figure 13) is thought to have permitted steady accumulation of ice at the polar caps and a particularly prolonged period of ice loss from the mid latitudes (Levrard et al., 2007; Smith et al., 2016).

While Mars' precise obliquity history is not well constrained beyond 20 Myr ago, the modelled ages and stratigraphy of mid-latitude ice deposits are broadly consistent with theoretical predictions. Based on a qualitative assessment of the youthful age of latitude-dependent mantle deposits, Head et al. (2003) proposed that they formed within the last few million years, with peaks of accumulation during excursions towards intermediate (~35°) obliquity, and a period of desiccation and degradation since ~400 kyr ago. This is in agreement with modelled ages of ~1–2 Myr for the mid-latitude portion of the LDM (e.g., Levy, Head, & Marchant, 2009b; Schon et al., 2012). The cyclic nature of deposition is consistent with observations of layering within the LDM. As suggested by early studies (e.g., Mellon & Jakosky, 1995), layers of subsurface ice could be preserved through low-obliquity episodes beneath protective lags of dust (e.g., Mellon and Jakosky, 1995; Head et al., 2003; Schon et al., 2009).

The older modelled ages of mid-latitude viscous flow features, on the order of hundreds of millions to 1 billion years, are consistent with their formation prior to the shift in Mars' average

obliquity ~5 Myr ago (Figure 13). While the precise obliquity solutions prior to 20 Myr ago are not known, statistically, the most likely obliquity over Mars' geologic history is ~40° (Laskar et al., 2004). This suggests that conditions similar to the 5–20 Myr period might have been more common throughout Mars history than those that have prevailed since 5 Myr ago. Indeed, mid-latitude glaciation on Mars might be a more typical state than polar glaciation.

Joining the Dots: Integrated Mapping of Ice Deposits and Potential for *In Situ* Resource Utilisation

It has long been recognised that water ice deposits in Mars' mid latitudes have potential as *in situ* resources for applications including rocket fuel production and life support systems for future crewed missions to the martian surface (e.g., Ramohalli et al., 1987; Paige, 1992; Mellon & Jakosky, 1993; Hoffman et al., 2017). Viscous flow features (putative debris-covered glaciers) in Mars' northern mid latitudes have been identified as prime targets among mid-latitude ice deposits (e.g., Hoffman et al., 2017; Baker & Carter, 2019a).

Morgan et al. (2021) noted that individual studies through the late 20th century and first two decades of the 21st century had focussed on specific areas or regions, on specific features, and/or on a limited range of datasets and techniques. Recognising the potential for a more integrated approach in planning for *in situ* resource utilisation, Morgan et al. (2021) and Putzig et al. (Submitted) began to join the dots. They combined datasets with suitable coverage for global-scale analyses, to produce an integrated subsurface water ice map (the 'SWIM' map) of Mars for areas <60°latitude and <1 km elevation (Figure 14). Areas above 1 km elevation are not included in the map because they are deemed as currently inaccessible to spacecraft which require aerobraking during descent through the atmosphere. The SWIM map describes the consistency of a range of techniques (neutron detections, thermal analyses, geomorphic mapping, and radar analyses of the surface and subsurface) with the presence of subsurface ice

in a given location. It broadly confirms the findings of earlier studies, and identifies the Deuteronilus Mensae, Arcadia Planitia, and Phlegra Montes regions of the northern hemisphere as particularly promising areas for *in situ* resource utilisation (Morgan et al., 2021).

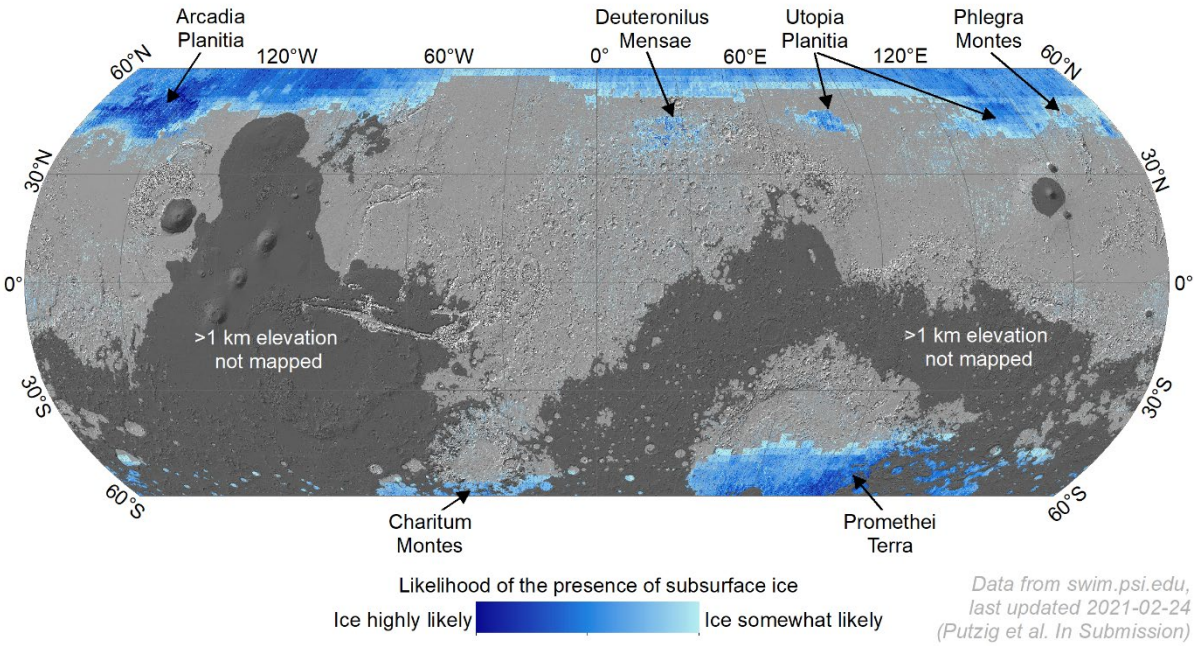

Figure 14: The SWIM 2.0 Combined Ice Consistency Map for latitudes <60° and elevations >1 km. *The colour scale is based on 'Combined Ice Consistency' (Ci) values 0.2≤Ci≤1 in the SWIM 2.0 combined ice consistency map from Putzig et al.* (Submitted). *See also Morgan et al.* (2021). *The basemap is a shaded relief map from MOLA topography.*

Image Credit: F. Butcher, with data from swim.psi.edu (last updated 24/02/2021).

Conclusions and Future Directions

Mars' mid latitudes host water ice in several forms, including as: shallow pore ice emplaced by vapour diffusion from the atmosphere; lenses of excess ice in the soil; extensive, thick buried layers of excess ice (perhaps with admixed dust); and high-purity debris-covered glaciers. Collectively, these deposits host ice in volumes equivalent to a global layer of water several metres thick. The majority of known subsurface ice deposits in Mars' mid latitudes are within

hundreds of metres of the present surface. Pore ice within the upper metres can be explained by vapour diffusion processes, but known excess ice deposits (which attain thicknesses of hundreds of metres in places) were likely derived from atmospheric precipitation of snow during cyclical excursions of Mars' obliquity up to ~35°, and subsequently buried by dust and debris. Deeper ice deposits (perhaps to depths of kilometres) might be present on Mars, including ice emplaced by freezing of deep groundwater within the regolith (e.g., Clifford et al., 2010). However, existing techniques are not well suited to the detection of such deposits.

A majority of the instruments deployed to study Mars' surface and subsurface during the second half of the 20th century and the first two decades of the 21st century were optimised for sensing to depths of less than ~1 m. Thus, the nature and distribution of ground ice at depths shallower than 1 m has been characterised by a variety of techniques. However, many of these techniques provide indirect observations, generalise near-surface properties over scales of kilometres to hundreds of kilometres, and/or require some assumptions to constrain ice properties. Constraints on the specific depth, configuration, and nature of near-surface ice in specific localities are limited to small (metres-wide) sites explored by the Phoenix lander (and to a lesser degree the Viking 2 lander), and happenstance excavations of substantial (i.e. larger than 25 cm) ice deposits, for example by small, fresh impact craters observed in the highest-resolution orbital images. Inferences about localised properties of near-surface ice elsewhere remain highly dependent upon numerical modelling and the interpretation of the metre-scale geomorphology of the surface using orbital images.

Studies of subsurface deposits to depths of hundreds of metres rely on a narrower range of datasets: orbital ground-penetrating radar and observations of the possible geomorphic and topographic signatures of these deposits at the surface. Nonetheless, abundant evidence has been found for extensive accumulations of thick, high-purity water ice buried to depths >1 m in Mars' mid latitudes, including direct imaging of natural exposures at a handful of locations.

The types of deep mid-latitude ice deposits identified to date can be broadly divided into three categories: (1) young (~5 Myr old) ice-rich mantling deposits termed the 'latitude-dependent mantle' (LDM) in Mars' mid-to-high latitudes (30–70°N, 25–65°S; Mustard et al., 2001; Head et al., 2003); (2) older (tens Myr) buried ice in plains regions such as Arcadia Planitia (e.g., Bramson et al. 2015) and Utopia Planitia (e.g. Stuurman et al. 2016); and (3) viscous flow features (10s Myr–1 billion year, typically 100s Myr old) thought to be analogous to debris-covered glaciers, which occur exclusively in Mars' mid latitudes (~30–60°N; Squyres, 1979; Levy et al., 2014).

A valuable addition to the datasets available to study Mars' mid-latitude ice deposits would be an orbital ground-penetrating radar capable of resolving the properties of the 1–20 m deep layer of the subsurface. Instruments deployed to Mars in the 20th century and the first two decades of the 21st century were unsuited for sensing these depths, and interpretations have been strongly dependent upon inferences from geomorphology, numerical modelling, and interpolation between shallow (<1 m) and deep (>20 m) detections. Characterisation of this intermediate layer will be essential for planning for future *in situ* resource utilisation by crewed missions to Mars, which would be likely to target excess ice deposits within this depth range. However, even crewed missions to Mars surface will be limited to relatively small exploration zones. Therefore, orbital remote sensing and numerical modelling techniques are likely to remain as keystones in our investigative toolset. Improvements in the coverage, resolution, and capabilities of orbital instruments, and the representation of complex physical processes (including aspects of Mars' subsurface and climate history which have not yet been constrained) in numerical models will be essential for the continued refinement of our understanding of water ice in Mars' mid latitudes.

Further Reading

Bell, J., (ed.) 2008, The Martian Surface: Composition Mineralogy and Physical Properties, Cambridge, UK: Cambridge University Press.

Carr, M.H., 2007, The Surface of Mars, Cambridge, UK: Cambridge University Press.

Conway, S.J., Carrivick, J.L., Carling, P.A., de Haas, T., Harrison, T.N., (eds.) 2019, Martian Gullies and their Earth Analogues, Geological Society, London, Special Publications, 467.

Filiberto, J., and Schwenzer, S.P., (eds.) 2018, Volatiles in the Martian Crust, Oxford, UK: Elsevier.

Haberle, R.M., Clancy, R.T., Forget, F., Smith, M.D. Zurek, R.W., (eds.) 2017, The Atmosphere and Climate of Mars, Cambridge, UK: Cambridge University Press.

References

Aharonson, O., & Schorghofer, N. (2006). Subsurface ice on Mars with rough topography. *Journal of Geophysical Research: Planets*, *111*(E11). https://doi.org/10.1029/2005JE002636

Arfstrom, J., & Hartmann, W. K. (2005). Martian flow features, moraine-like ridges, and gullies: Terrestrial analogs and interrelationships. *Icarus*, *174*(2), 321–335. https://doi.org/10.1016/j.icarus.2004.05.026

Baker, D. M. H., & Head, J. W. (2015). Extensive Middle Amazonian mantling of debris aprons and plains in Deuteronilus Mensae, Mars: Implications for the record of mid-latitude glaciation. *Icarus*, *260*, 269–288. https://doi.org/10.1016/j.icarus.2015.06.036

Baker, D. M. H., & Carter, L. M. (2019a). Probing supraglacial debris on Mars 1: Sources, thickness, and stratigraphy. *Icarus*, *319*, 745–769. https://doi.org/10.1016/j.icarus.2018.09.001

Baker, D. M. H., & Carter, L. M. (2019b). Probing supraglacial debris on Mars 2: Crater morphology. *Icarus*, *319*, 264–280. https://doi.org/10.1016/j.icarus.2018.09.009

Bandfield, J. L. (2007). High-resolution subsurface water-ice distributions on Mars. *Nature*, *447*(7140), 64–67. https://doi.org/10.1038/nature05781

Bandfield, J. L., & Feldman, W. C. (2008). Martian high latitude permafrost depth and surface cover thermal inertia distributions. *Journal of Geophysical Research: Planets*, *113*(E8). https://doi.org/10.1029/2007JE003007

Baumann, A. (1909). Erklärung der Oberfläche des Planeten Mars. *Wissen Und Leben*, *5*, 574–579. https://doi.org/10.5169/seals-750919

Berman, D. C., Chuang, F. C., Smith, I. B., & Crown, D. A. (2021). Ice-rich landforms of the southern mid-latitudes of Mars: A case study in Nereidum Montes. *Icarus*, *355*, 114170. https://doi.org/10.1016/j.icarus.2020.114170

Boynton, W. V., Feldman, W. C., Mitrofanov, I. G., Evans, L. G., Reedy, R. C., Squyres, S. W., Starr, R., Trombka, J. I., d'Uston, C., Arnold, J. R., Englert, P. A. J., Metzger, A. E., Wänke, H., Brückner, J., Drake, D. M., Shinohara, C., Fellows, C., Hamara, D. K., Harshman, K., … Ton'chev, A. K. (2004). The Mars Odyssey Gamma-Ray Spectrometer Instrument Suite. *Space Science Reviews*, *110*(1), 37–83. https://doi.org/10.1023/B:SPAC.0000021007.76126.15

Boynton, W. V., Feldman, W. C., Squyres, S. W., Prettyman, T. H., Brückner, J., Evans, L. G., Reedy, R. C., Starr, R., Arnold, J. R., Drake, D. M., Englert, P. a. J., Metzger, A. E., Mitrofanov, I., Trombka, J. I., d'Uston, C., Wänke, H., Gasnault, O., Hamara, D. K., Janes, D. M., … Shinohara, C. (2002). Distribution of Hydrogen in the Near Surface of Mars: Evidence for Subsurface Ice Deposits. *Science*, *297*(5578), 81–85. https://doi.org/10.1126/science.1073722

Bramson, A. M., Byrne, S., Putzig, N. E., Sutton, S., Plaut, J. J., Brothers, T. C., & Holt, J. W. (2015). Widespread excess ice in Arcadia Planitia, Mars. *Geophysical Research Letters*, *42*(16), 6566–6574. https://doi.org/10.1002/2015GL064844

Brough, S., Hubbard, B., & Hubbard, A. (2016). Former extent of glacier-like forms on Mars. *Icarus*, *274*, 37–49. https://doi.org/10.1016/j.icarus.2016.03.006

Brough, S., Hubbard, B., Souness, C., Grindrod, P. M., & Davis, J. (2015). Landscapes of polyphase glaciation: eastern Hellas Planitia, Mars. *Journal of Maps*, 1–13. https://doi.org/10.1080/17445647.2015.1047907

Brough, S., Hubbard, B., & Hubbard, A. (2019). Area and volume of mid-latitude glacier-like forms on Mars. *Earth and Planetary Science Letters*, *507*, 10–20. https://doi.org/10.1016/j.epsl.2018.11.031

Butcher, F. E. G. (2019). *Wet-Based Glaciation on Mars* [PhD Thesis]. The Open University.

Butcher, F. E. G., Balme, M. R., Conway, S. J., Gallagher, C., Arnold, N. S., Storrar, R. D., Lewis, S. R., & Hagermann, A. (2020). Morphometry of a glacier-linked esker in NW Tempe Terra, Mars, and implications for sediment-discharge dynamics of subglacial drainage. *Earth and Planetary Science Letters*, *542*, 116325. https://doi.org/10.1016/j.epsl.2020.116325

Butcher, F. E. G., Balme, M. R., Gallagher, C., Arnold, N. S., Conway, S. J., Hagermann, A., & Lewis, S. R. (2017). Recent Basal Melting of a Mid-Latitude Glacier on Mars. *Journal of Geophysical Research: Planets*, *122*(12), 2445–2468. https://doi.org/10.1002/2017JE005434

Butcher, F. E. G., Balme, M. R., Conway, S. J., Gallagher, C., Arnold, N. S., Storrar, R. D., Lewis, S. R., Hagermann, A., & Davis, J. M. (2021). Sinuous ridges in Chukhung crater, Tempe Terra, Mars: Implications for fluvial, glacial, and glaciofluvial activity. *Icarus*, *357*, 114131. https://doi.org/10.1016/j.icarus.2020.114131

Byrne, S., Dundas, C. M., Kennedy, M. R., Mellon, M. T., McEwen, A. S., Cull, S. C., Daubar, I. J., Shean, D. E., Seelos, K. D., Murchie, S. L., Cantor, B. A., Arvidson, R. E., Edgett, K. S., Reufer, A., Thomas, N., Harrison, T. N., Posiolova, L. V., & Seelos, F. P. (2009). Distribution of Mid-Latitude Ground Ice on Mars from New Impact Craters. *Science*, *325*(5948), 1674–1676. https://doi.org/10.1126/science.1175307

Cabrol, N. A. (2021). Tracing a modern biosphere on Mars. *Nature Astronomy*, *5*(3), 210–212. https://doi.org/10.1038/s41550-021-01327-x

Campbell, B. A., & Morgan, G. A. (2018). Fine-Scale Layering of Mars Polar Deposits and Signatures of Ice Content in Nonpolar Material From Multiband SHARAD Data Processing. *Geophysical Research Letters*, *45*(4), 1759–1766. https://doi.org/10.1002/2017GL075844

Carr, M. H., & Schaber, G. G. (1977). Martian permafrost features. *Journal of Geophysical Research*, *82*(28), 4039–4054. https://doi.org/10.1029/JS082i028p04039

Christensen, P. R. (2003). Formation of recent martian gullies through melting of extensive water-rich snow deposits. *Nature*, *422*(6927), 45–48. https://doi.org/10.1038/nature01436

Clifford, S. M., Lasue, J., Heggy, E., Boisson, J., McGovern, P., & Max, M. D. (2010). Depth of the Martian cryosphere: Revised estimates and implications for the existence and detection of subpermafrost groundwater. *Journal of Geophysical Research: Planets*, *115*(E7), E07001. https://doi.org/10.1029/2009JE003462

Clifford, S. M. (1991). The role of thermal vapor diffusion in the subsurface hydrologic evolution of Mars. *Geophysical Research Letters*, *18*(11), 2055–2058. https://doi.org/10.1029/91GL02469

Clifford, S. M., & Hillel, D. (1983). The stability of ground ice in the equatorial region of Mars. *Journal of Geophysical Research: Solid Earth*, *88*(B3), 2456–2474. https://doi.org/10.1029/JB088iB03p02456

Colaprete, A., & Jakosky, B. M. (1998). Ice flow and rock glaciers on Mars. *Journal of Geophysical Research: Planets*, *103*(E3), 5897–5909. https://doi.org/10.1029/97JE03371

Conway, S. J., & Balme, M. R. (2014). Decameter thick remnant glacial ice deposits on Mars. *Geophysical Research Letters*, *41*(15), 5402–5409. https://doi.org/10.1002/2014GL060314

Conway, S. J., de Haas, T., & Harrison, T. N. (2018). Martian gullies: a comprehensive review of observations, mechanisms and insights from Earth analogues. *Geological Society, London, Special Publications*, *467*, 7–66. https://doi.org/10.1144/SP467.14

Conway, S. J., & Mangold, N. (2013). Evidence for Amazonian mid-latitude glaciation on Mars from impact crater asymmetry. *Icarus*, *225*(1), 413–423. https://doi.org/10.1016/j.icarus.2013.04.013

Costard, F., Forget, F., Mangold, N., & Peulvast, J. P. (2002). Formation of Recent Martian Debris Flows by Melting of Near-Surface Ground Ice at High Obliquity. *Science*, *295*(5552), 110–113. https://doi.org/10.1126/science.1066698

Costard, F. M., & Kargel, J. S. (1995). Outwash Plains and Thermokarst on Mars. *Icarus*, *114*(1), 93–112. https://doi.org/10.1006/icar.1995.1046

Dickson, J. L., Head, J. W., & Fassett, C. I. (2012). Patterns of accumulation and flow of ice in the mid-latitudes of Mars during the Amazonian. *Icarus*, *219*(2), 723–732. https://doi.org/10.1016/j.icarus.2012.03.010

Dickson, J. L., Head, J. W., & Marchant, D. R. (2008). Late Amazonian glaciation at the dichotomy boundary on Mars: Evidence for glacial thickness maxima and multiple glacial phases. *Geology*, *36*(5), 411–414. https://doi.org/10.1130/G24382A.1

Dickson, J. L., Head, J. W., & Marchant, D. R. (2010). Kilometer-thick ice accumulation and glaciation in the northern mid-latitudes of Mars: Evidence for crater-filling events in the Late Amazonian at the Phlegra Montes. *Earth and Planetary Science Letters*, *294*(3–4), 332–342. https://doi.org/10.1016/j.epsl.2009.08.031

Diniega, S., Byrne, S., Bridges, N. T., Dundas, C. M., & McEwen, A. S. (2010). Seasonality of present-day Martian dune-gully activity. *Geology*, *38*(11), 1047–1050. https://doi.org/10.1130/G31287.1

Dundas, C. M., Bramson, A. M., Ojha, L., Wray, J. J., Mellon, M. T., Byrne, S., McEwen, A. S., Putzig, N. E., Viola, D., Sutton, S., Clark, E., & Holt, J. W. (2018). Exposed subsurface ice sheets in the Martian mid-latitudes. *Science*, *359*(6372), 199–201. https://doi.org/10.1126/science.aao1619

Dundas, C. M., Byrne, S., & McEwen, A. S. (2015). Modeling the development of martian sublimation thermokarst landforms. *Icarus*, *262*, 154–169. https://doi.org/10.1016/j.icarus.2015.07.033

Dundas, C. M., Byrne, S., McEwen, A. S., Mellon, M. T., Kennedy, M. R., Daubar, I. J., & Saper, L. (2014). HiRISE observations of new impact craters exposing Martian ground ice. *Journal of Geophysical Research: Planets*, *119*(1), 109–127. https://doi.org/10.1002/2013JE004482

Dundas, C. M., McEwen, A. S., Diniega, S., Byrne, S., & Martinez-Alonso, S. (2010). New and recent gully activity on Mars as seen by HiRISE. *Geophysical Research Letters*, *37*(7), L07202. https://doi.org/10.1029/2009GL041351

Dundas, C. M., Mellon, M. T., Conway, S. J., Daubar, I. J., Williams, K. E., Ojha, L., Wray, J. J., Bramson, A. M., Byrne, S., McEwen, A. S., Posiolova, L. V., Speth, G., Viola, D., Landis, M. E., Morgan, G. A., & Pathare, A. V. (2021). Widespread Exposures of Extensive Clean Shallow Ice in the Midlatitudes of Mars. *Journal of Geophysical Research: Planets*, *126*(3), e2020JE006617. https://doi.org/10.1029/2020JE006617

Fanale, F. P. (1976). Martian volatiles: Their degassing history and geochemical fate. *Icarus*, *28*(2), 179–202. https://doi.org/10.1016/0019-1035(76)90032-4

Fanale, F. P., Salvail, J. R., Zent, A. P., & Postawko, S. E. (1986). Global distribution and migration of subsurface ice on Mars. *Icarus*, *67*(1), 1–18. https://doi.org/10.1016/0019-1035(86)90170-3

Farmer, C. B., & Doms, P. E. (1979). Global seasonal variation of water vapor on Mars and the implications for permafrost. *Journal of Geophysical Research: Solid Earth*, *84*(B6), 2881–2888. https://doi.org/10.1029/JB084iB06p02881

Fassett, C. I., Dickson, J. L., Head, J. W., Levy, J. S., & Marchant, D. R. (2010). Supraglacial and proglacial valleys on Amazonian Mars. *Icarus*, *208*(1), 86–100. https://doi.org/10.1016/j.icarus.2010.02.021

Fastook, J. L., & Head, J. W. (2014). Amazonian mid- to high-latitude glaciation on Mars: Supply-limited ice sources, ice accumulation patterns, and concentric crater fill glacial flow and ice sequestration. *Planetary and Space Science*, *91*, 60–76. https://doi.org/10.1016/j.pss.2013.12.002

Feldman, W. C., Prettyman, T. H., Maurice, S., Plaut, J. J., Bish, D. L., Vaniman, D. T., Mellon, M. T., Metzger, A. E., Squyres, S. W., Karunatillake, S., Boynton, W. V., Elphic, R. C., Funsten, H. O., Lawrence, D. J., & Tokar, R. L. (2004). Global distribution of near-surface hydrogen on Mars. *Journal of Geophysical Research: Planets*, *109*(E9), E09006. https://doi.org/10.1029/2003JE002160

Feldman, W. C., Pathare, A., Maurice, S., Prettyman, T. H., Lawrence, D. J., Milliken, R. E., & Travis, B. J. (2011). Mars Odyssey neutron data: 2. Search for buried excess water ice deposits at nonpolar latitudes on Mars. *Journal of Geophysical Research: Planets*, *116*(E11). https://doi.org/10.1029/2011JE003806

Forget, F., Haberle, R. M., Montmessin, F., Levrard, B., & Head, J. W. (2006). Formation of Glaciers on Mars by Atmospheric Precipitation at High Obliquity. *Science*, *311*(5759), 368–371. https://doi.org/10.1126/science.1120335

Gallagher, C., & Balme, M. (2015). Eskers in a complete, wet-based glacial system in the Phlegra Montes region, Mars. *Earth and Planetary Science Letters*, *431*, 96–109. https://doi.org/10.1016/j.epsl.2015.09.023

Gallagher, C., Butcher, F. E. G., Balme, M., Smith, I., & Arnold, N. (2021). Landforms indicative of regional warm based glaciation, Phlegra Montes, Mars. *Icarus*, *355*, 114173. https://doi.org/10.1016/j.icarus.2020.114173

Gatto, L. W., & Anderson, D. M. (1975). Alaskan Thermokarst Terrain and Possible Martian Analog. *Science*, *188*(4185), 255–257. https://doi.org/10.1126/science.188.4185.255

Harish, Vijayan, S., Mangold, N., & Bhardwaj, A. (2020). Water-Ice Exposing Scarps Within the Northern Midlatitude Craters on Mars. *Geophysical Research Letters*, *47*(14), e2020GL089057. https://doi.org/10.1029/2020GL089057

Hartmann, W. K. (2005). Martian cratering 8: Isochron refinement and the chronology of Mars. *Icarus*, *174*(2), 294–320. https://doi.org/10.1016/j.icarus.2004.11.023

Hartmann, W. K., Ansan, V., Berman, D. C., Mangold, N., & Forget, F. (2014). Comprehensive analysis of glaciated martian crater Greg. *Icarus*, *228*, 96–120. https://doi.org/10.1016/j.icarus.2013.09.016

Hartmann, W. K., & Neukum, G. (2001). Cratering Chronology and the Evolution of Mars. *Space Science Reviews*, *96*(1–4), 165–194. https://doi.org/10.1023/A:1011945222010

Hauber, E., Gasselt, S. van, Chapman, M. G., & Neukum, G. (2008). Geomorphic evidence for former lobate debris aprons at low latitudes on Mars: Indicators of the Martian paleoclimate. *Journal of Geophysical Research: Planets*, *113*(E2), E02007. https://doi.org/10.1029/2007JE002897

Head, J. W., Marchant, D. R., Agnew, M. C., Fassett, C. I., & Kreslavsky, M. A. (2006). Extensive valley glacier deposits in the northern mid-latitudes of Mars: Evidence for Late Amazonian obliquity-driven climate change. *Earth and Planetary Science Letters*, *241*(3–4), 663–671. https://doi.org/10.1016/j.epsl.2005.11.016

Head, J. W., Marchant, D. R., Dickson, J. L., Kress, A. M., & Baker, D. M. (2010). Northern mid-latitude glaciation in the Late Amazonian period of Mars: Criteria for the recognition of debris-covered glacier and valley glacier landsystem deposits. *Earth and Planetary Science Letters*, *294*(3–4), 306–320. https://doi.org/10.1016/j.epsl.2009.06.041

Head, J. W., Mustard, J. F., Kreslavsky, M. A., Milliken, R. E., & Marchant, D. R. (2003). Recent ice ages on Mars. *Nature*, *426*(6968), 797–802. https://doi.org/10.1038/nature02114

Head, J. W., Neukum, G., Jaumann, R., Hiesinger, H., Hauber, E., Carr, M., Masson, P., Foing, B., Hoffmann, H., Kreslavsky, M., Werner, S., Milkovich, S., van Gasselt, S., & The HRSC Co-Investigator Team. (2005). Tropical to mid-latitude snow and ice accumulation, flow and glaciation on Mars. *Nature*, *434*(7031), 346–351. https://doi.org/10.1038/nature03359

Hecht, M. H. (2002). Metastability of liquid water on Mars. *Icarus*, *156*(2), 373–386. https://doi.org/10.1006/icar.2001.6794

Hepburn, A. J., Ng, F. S. L., Holt, T. O., & Hubbard, B. (2020). Late Amazonian Ice Survival in Kasei Valles, Mars. *Journal of Geophysical Research: Planets*, *125*(11), e2020JE006531. https://doi.org/10.1029/2020JE006531

Hepburn, A. J., Ng, F. S. L., Livingstone, S. J., Holt, T. O., & Hubbard, B. (2020). Polyphase Mid-Latitude Glaciation on Mars: Chronology of the Formation of Superposed Glacier-Like Forms from Crater-Count Dating. *Journal of Geophysical Research: Planets*, *125*(2), e2019JE006102. https://doi.org/10.1029/2019JE006102

Herschel, W. (1784). XIX. On the remarkable appearances at the polar regions of the planet Mars, and its spheroidical figure; with a few hints relating to its real diameter and atmosphere. *Philosophical Transactions of the Royal Society of London*, *74*, 233–273. https://doi.org/10.1098/rstl.1784.0020

Hobley, D. E. J., Howard, A. D., & Moore, J. M. (2014). Fresh shallow valleys in the Martian midlatitudes as features formed by meltwater flow beneath ice. *Journal of Geophysical Research: Planets*, *119*(1), 128–153. https://doi.org/10.1002/2013JE004396

Hoffman, N. (2002). Active Polar Gullies on Mars and the Role of Carbon Dioxide. *Astrobiology*, *2*(3), 313–323. https://doi.org/10.1089/153110702762027899

Hoffman, S. J., Andrews, A., Joosten, B. K., & Watts, K. (2017). A water rich mars surface mission scenario. *2017 IEEE Aerospace Conference*, 1–21. https://doi.org/10.1109/AERO.2017.7943911

Holt, J. W., Safaeinili, A., Plaut, J. J., Head, J. W., Phillips, R. J., Seu, R., Kempf, S. D., Choudhary, P., Young, D. A., Putzig, N. E., Biccari, D., & Gim, Y. (2008). Radar Sounding Evidence for Buried Glaciers in the Southern Mid-Latitudes of Mars. *Science*, *322*(5905), 1235–1238. https://doi.org/10.1126/science.1164246

Hubbard, B., Milliken, R. E., Kargel, J. S., Limaye, A., & Souness, C. (2011). Geomorphological characterisation and interpretation of a mid-latitude glacier-like

form: Hellas Planitia, Mars. *Icarus*, *211*(1), 330–346. https://doi.org/10.1016/j.icarus.2010.10.021

Ivanov, B. A. (2001). Mars/Moon Cratering Rate Ratio Estimates. *Space Science Reviews*, *96*(1–4), 87–104. https://doi.org/10.1023/A:1011941121102

Jaumann, R., Neukum, G., Behnke, T., Duxbury, T. C., Eichentopf, K., Flohrer, J., Gasselt, S. v., Giese, B., Gwinner, K., Hauber, E., Hoffmann, H., Hoffmeister, A., Köhler, U., Matz, K.-D., McCord, T. B., Mertens, V., Oberst, J., Pischel, R., Reiss, D., … Wählisch, M. (2007). The high-resolution stereo camera (HRSC) experiment on Mars Express: Instrument aspects and experiment conduct from interplanetary cruise through the nominal mission. *Planetary and Space Science*, *55*(7–8), 928–952. https://doi.org/10.1016/j.pss.2006.12.003

Kadish, S. J., Head, J. W., Parsons, R. L., & Marchant, D. R. (2008). The Ascraeus Mons fan-shaped deposit: Volcano–ice interactions and the climatic implications of cold-based tropical mountain glaciation. *Icarus*, *197*(1), 84–109. https://doi.org/10.1016/j.icarus.2008.03.019

Khuller, A. R., & Christensen, P. R. (2021). Evidence of Exposed Dusty Water Ice within Martian Gullies. *Journal of Geophysical Research: Planets*, *126*(2), e2020JE006539. https://doi.org/10.1029/2020JE006539

Kliore, A., Cain, D. L., Levy, G. S., Eshleman, V. R., Fjeldbo, G., & Drake, F. D. (1965). Occultation Experiment: Results of the First Direct Measurement of Mars's Atmosphere and Ionosphere. *Science*, *149*(3689), 1243–1248. https://doi.org/10.1126/science.149.3689.1243

Knauth, L. P. (2000). Ideas About the Surface Runoff Features on Mars. *Science*, *290*(5492), 711–712. https://doi.org/10.1126/science.290.5492.711c

Kochel, R. C., & Peake, R. T. (1984). Quantification of waste morphology in Martian fretted terrain. *Journal of Geophysical Research: Solid Earth*, *89*(S01), C336–C350. https://doi.org/10.1029/JB089iS01p0C336

Kostama, V.-P., Kreslavsky, M. A., & Head, J. W. (2006). Recent high-latitude icy mantle in the northern plains of Mars: Characteristics and ages of emplacement. *Geophysical Research Letters*, *33*(11), L11201. https://doi.org/10.1029/2006GL025946

Kreslavsky, M. A., & Head, J. W. (2000). Kilometer-scale roughness of Mars: Results from MOLA data analysis. *Journal of Geophysical Research-Planets*, *105*(E11), 26695–26711. https://doi.org/10.1029/2000JE001259

Kreslavsky, M. A., & Head, J. W. (2002). Mars: Nature and evolution of young latitude-dependent water-ice-rich mantle. *Geophysical Research Letters*, *29*(15), 1719. https://doi.org/10.1029/2002GL015392

Kuzmin, R. O., Zabalueva, E. V., Mitrofanov, I. G., Litvak, M. L., Boynton, W. V., & Saunders, R. S. (2004). Regions of Potential Existence of Free Water (Ice) in the Near-Surface Martian Ground: Results from the Mars Odyssey High-Energy Neutron Detector (HEND). *Solar System Research*, *38*(1), 1–11. https://doi.org/10.1023/B:SOLS.0000015150.61420.5b

Laskar, J., Correia, A. C. M., Gastineau, M., Joutel, F., Levrard, B., & Robutel, P. (2004). Long term evolution and chaotic diffusion of the insolation quantities of Mars. *Icarus*, *170*(2), 343–364. https://doi.org/10.1016/j.icarus.2004.04.005

Laskar, J., Joutel, F., & Boudin, F. (1993). Orbital, Precessional, and Insolation Quantities for the Earth from -20 Myr to +10 Myr. *Astronomy & Astrophysics*, *270*(1–2), 522–533.

Laskar, J., & Robutel, P. (1993). The chaotic obliquity of the planets. *Nature*, *361*(6413), 608–612. https://doi.org/10.1038/361608a0

Lederberg, J., & Sagan, C. (1962). Microenvironments for Life on Mars. *Proceedings of the National Academy of Sciences of the United States of America*, *48*(9), 1473–1475.

Lefort, A., Russell, P. S., & Thomas, N. (2010). Scalloped terrains in the Peneus and Amphitrites Paterae region of Mars as observed by HiRISE. *Icarus*, *205*(1), 259–268. https://doi.org/10.1016/j.icarus.2009.06.005

Lefort, A., Russell, P. S., Thomas, N., McEwen, A. S., Dundas, C. M., & Kirk, R. L. (2009). Observations of periglacial landforms in Utopia Planitia with the High Resolution Imaging Science Experiment (HiRISE). *Journal of Geophysical Research: Planets*, *114*(E4). https://doi.org/10.1029/2008JE003264

Leighton, R. B., Horowitz, N. H., Murray, B. C., Sharp, R. P., Herriman, A. H., Young, A. T., Smith, B. A., Davies, M. E., & Leovy, C. B. (1969). Mariner 6 and 7 Television Pictures: Preliminary Analysis. *Science*, *166*(3901), 49–67. https://doi.org/10.1126/science.166.3901.49

Leighton, R. B., & Murray, B. C. (1966). Behavior of Carbon Dioxide and Other Volatiles on Mars. *Science*, *153*(3732), 136–144. https://doi.org/10.1126/science.153.3732.136

Leighton, R. B., Murray, B. C., Sharp, R. P., Allen, J. D., & Sloan, R. K. (1965). Mariner IV Photography of Mars: Initial Results. *Science*, *149*(3684), 627–630. https://doi.org/10.1126/science.149.3684.627

Levrard, B., Forget, F., Montmessin, F., & Laskar, J. (2004). Recent ice-rich deposits formed at high latitudes on Mars by sublimation of unstable equatorial ice during low obliquity. *Nature*, *431*(7012), 1072–1075. https://doi.org/10.1038/nature03055

Levrard, B., Forget, F., Montmessin, F., & Laskar, J. (2007). Recent formation and evolution of northern Martian polar layered deposits as inferred from a Global Climate Model. *Journal of Geophysical Research: Planets*, *112*(E6), E06012. https://doi.org/10.1029/2006JE002772

Levy, J. S., Fassett, C. I., Head, J. W., Schwartz, C., & Watters, J. L. (2014). Sequestered glacial ice contribution to the global Martian water budget: Geometric constraints on the volume of remnant, midlatitude debris-covered glaciers. *Journal of Geophysical Research: Planets*, *119*(10), 2188–2196. https://doi.org/10.1002/2014JE004685

Levy, J. S., Head, J., & Marchant, D. (2009a). Thermal contraction crack polygons on Mars: Classification, distribution, and climate implications from HiRISE observations. *Journal of Geophysical Research: Planets*, *114*(E1). https://doi.org/10.1029/2008JE003273

Levy, J. S., Head, J. W., & Marchant, D. R. (2007). Lineated valley fill and lobate debris apron stratigraphy in Nilosyrtis Mensae, Mars: Evidence for phases of glacial modification of the dichotomy boundary. *Journal of Geophysical Research: Planets*, *112*(E8), E08004. https://doi.org/10.1029/2006JE002852

Levy, J. S., Head, J. W., & Marchant, D. R. (2009b). Concentric crater fill in Utopia Planitia: History and interaction between glacial "brain terrain" and periglacial mantle processes. *Icarus*, *202*(2), 462–476. https://doi.org/10.1016/j.icarus.2009.02.018

Levy, J. S., Head, J. W., & Marchant, D. R. (2010). Concentric crater fill in the northern mid-latitudes of Mars: Formation processes and relationships to similar landforms of glacial origin. *Icarus*, *209*(2), 390–404. https://doi.org/10.1016/j.icarus.2010.03.036

Levy, J. S., Head, J. W., Marchant, D. R., Dickson, J. L., & Morgan, G. A. (2009). Geologically recent gully–polygon relationships on Mars: Insights from the Antarctic Dry Valleys on the roles of permafrost, microclimates, and water sources for surface flow. *Icarus*, *201*(1), 113–126. https://doi.org/10.1016/j.icarus.2008.12.043

Levy, J. S., Marchant, D. R., & Head, J. W. (2010). Thermal contraction crack polygons on Mars: A synthesis from HiRISE, Phoenix, and terrestrial analog studies. *Icarus*, *206*(1), 229–252. https://doi.org/10.1016/j.icarus.2009.09.005

Lucchitta, B. K. (1981). Mars and Earth: Comparison of cold-climate features. *Icarus*, *45*(2), 264–303. https://doi.org/10.1016/0019-1035(81)90035-X

Lucchitta, B. K. (1984). Ice and debris in the Fretted Terrain, Mars. *Journal of Geophysical Research: Solid Earth*, *89*(S02), B409–B418. https://doi.org/10.1029/JB089iS02p0B409

Madeleine, J.-B., Forget, F., Head, J. W., Levrard, B., Montmessin, F., & Millour, E. (2009). Amazonian northern mid-latitude glaciation on Mars: A proposed climate scenario. *Icarus*, *203*(2), 390–405. https://doi.org/10.1016/j.icarus.2009.04.037

Malakhov, A. V., Mitrofanov, I. G., Litvak, M. L., Sanin, A. B., Golovin, D. V., Djachkova, M. V., Nikiforov, S. Y., Anikin, A. A., Lisov, D. I., Lukyanov, N. V., & Mokrousov, M. I. (2020). Ice Permafrost '"Oases"' Close to Martian Equator: Planet Neutron Mapping Based on Data of FREND Instrument Onboard TGO Orbiter of Russian-European ExoMars Mission. *Astronomy Letters*, *46*(6), 407–421. https://doi.org/10.1134/S1063773720060079

Malin, M. C., Bell, J. F., Cantor, B. A., Caplinger, M. A., Calvin, W. M., Clancy, R. T., Edgett, K. S., Edwards, L., Haberle, R. M., James, P. B., Lee, S. W., Ravine, M. A., Thomas, P. C., & Wolff, M. J. (2007). Context Camera Investigation on board the Mars Reconnaissance Orbiter. *Journal of Geophysical Research: Planets*, *112*(E5), E05S04. https://doi.org/10.1029/2006JE002808

Malin, M. C., & Edgett, K. S. (2000). Evidence for Recent Groundwater Seepage and Surface Runoff on Mars. *Science*, *288*(5475), 2330–2335. https://doi.org/10.1126/science.288.5475.2330

Malin, M. C., & Edgett, K. S. (2001). Mars Global Surveyor Mars Orbiter Camera: Interplanetary cruise through primary mission. *Journal of Geophysical Research: Planets*, *106*(E10), 23429–23570. https://doi.org/10.1029/2000JE001455

Malin, M. C., Edgett, K. S., Posiolova, L. V., McColley, S. M., & Dobrea, E. Z. N. (2006). Present-Day Impact Cratering Rate and Contemporary Gully Activity on Mars. *Science*, *314*(5805), 1573–1577. https://doi.org/10.1126/science.1135156

Mangold, N. (2003). Geomorphic analysis of lobate debris aprons on Mars at Mars Orbiter Camera scale: Evidence for ice sublimation initiated by fractures. *Journal of Geophysical Research: Planets*, *108*(E4), 8021. https://doi.org/10.1029/2002JE001885

Mangold, N., & Allemand, P. (2001). Topographic analysis of features related to ice on Mars. *Geophysical Research Letters*, *28*(3), 407–410. https://doi.org/10.1029/2000GL008491

Mangold, N., Allemand, P., Duval, P., Geraud, Y., & Thomas, P. (2002). Experimental and theoretical deformation of ice–rock mixtures: Implications on rheology and ice content of Martian permafrost. *Planetary and Space Science*, *50*(4), 385–401. https://doi.org/10.1016/S0032-0633(02)00005-3

Mangold, N., Maurice, S., Feldman, W. C., Costard, F., & Forget, F. (2004). Spatial relationships between patterned ground and ground ice detected by the Neutron Spectrometer on Mars. *Journal of Geophysical Research: Planets*, *109*(E8), E08001. https://doi.org/10.1029/2004JE002235

Martellato, E., Bramson, A. M., Cremonese, G., Lucchetti, A., Marzari, F., Massironi, M., Re, C., & Byrne, S. (2020). Martian Ice Revealed by Modeling of Simple Terraced Crater Formation. *Journal of Geophysical Research: Planets*, *125*(10), e2019JE006108. https://doi.org/10.1029/2019JE006108

McCauley, J. F., Carr, M. H., Cutts, J. A., Hartmann, W. K., Masursky, H., Milton, D. J., Sharp, R. P., & Wilhelms, D. E. (1972). Preliminary mariner 9 report on the geology of Mars. *Icarus*, *17*(2), 289–327. https://doi.org/10.1016/0019-1035(72)90003-6

McCleese, D. J., Schofield, J. T., Taylor, F. W., Calcutt, S. B., Foote, M. C., Kass, D. M., Leovy, C. B., Paige, D. A., Read, P. L., & Zurek, R. W. (2007). Mars Climate Sounder: An investigation of thermal and water vapor structure, dust and condensate distributions in the atmosphere, and energy balance of the polar regions. *Journal of Geophysical Research: Planets*, *112*(E5). https://doi.org/10.1029/2006JE002790

McEwen, A. S., Eliason, E. M., Bergstrom, J. W., Bridges, N. T., Hansen, C. J., Delamere, W. A., Grant, J. A., Gulick, V. C., Herkenhoff, K. E., Keszthelyi, L., Kirk, R. L., Mellon, M. T., Squyres, S. W., Thomas, N., & Weitz, C. M. (2007). Mars Reconnaissance Orbiter's High Resolution Imaging Science Experiment (HiRISE). *Journal of Geophysical Research*, *112*(E5), E05S02. https://doi.org/10.1029/2005JE002605

Mellon, M. T., & Jakosky, B. M. (1995). The distribution and behavior of Martian ground ice during past and present epochs. *Journal of Geophysical Research: Planets*, *100*(E6), 11781–11799. https://doi.org/10.1029/95JE01027

Mellon, M. T., Arvidson, R. E., Sizemore, H. G., Searls, M. L., Blaney, D. L., Cull, S., Hecht, M. H., Heet, T. L., Keller, H. U., Lemmon, M. T., Markiewicz, W. J., Ming, D. W., Morris, R. V., Pike, W. T., & Zent, A. P. (2009). Ground ice at the Phoenix Landing Site: Stability state and origin. *Journal of Geophysical Research: Planets*, *114*(E1), E00E07. https://doi.org/10.1029/2009JE003417

Mellon, M. T., Feldman, W. C., & Prettyman, T. H. (2004). The presence and stability of ground ice in the southern hemisphere of Mars. *Icarus*, *169*(2), 324–340. https://doi.org/10.1016/j.icarus.2003.10.022

Mellon, M. T., & Jakosky, B. M. (1993). Geographic variations in the thermal and diffusive stability of ground ice on Mars. *Journal of Geophysical Research: Planets*, *98*(E2), 3345–3364. https://doi.org/10.1029/92JE02355

Mest, S. C., & Crown, D. A. (2001). Geology of the Reull Vallis Region, Mars. *Icarus*, *153*(1), 89–110. https://doi.org/10.1006/icar.2001.6655

Michael, G. G., Platz, T., Kneissl, T., & Schmedemann, N. (2012). Planetary surface dating from crater size–frequency distribution measurements: Spatial randomness and clustering. *Icarus*, *218*(1), 169–177. https://doi.org/10.1016/j.icarus.2011.11.033

Milliken, R. E., Mustard, J. F., & Goldsby, D. L. (2003). Viscous flow features on the surface of Mars: Observations from high-resolution Mars Orbiter Camera (MOC) images. *Journal of Geophysical Research: Planets*, *108*(E6), 5057. https://doi.org/10.1029/2002JE002005

Mischna, M. A., Richardson, M. I., Wilson, R. J., & McCleese, D. J. (2003). On the orbital forcing of Martian water and CO2 cycles: A general circulation model study with simplified volatile schemes. *Journal of Geophysical Research: Planets*, *108*(E6). https://doi.org/10.1029/2003JE002051

Mitrofanov, I. G., Litvak, M. L., Kozyrev, A. S., Sanin, A. B., Tret'yakov, V. I., Grin'kov, V. Y., Boynton, W. V., Shinohara, C., Hamara, D., & Saunders, R. S. (2004). Soil Water Content on Mars as Estimated from Neutron Measurements by the HEND Instrument Onboard the 2001 Mars Odyssey Spacecraft. *Solar System Research*, *38*(4), 253–257. https://doi.org/10.1023/B:SOLS.0000037461.70809.45

Mitrofanov, I., Malakhov, A., Bakhtin, B., Golovin, D., Kozyrev, A., Litvak, M., Mokrousov, M., Sanin, A., Tretyakov, V., Vostrukhin, A., Anikin, A., Zelenyi, L. M., Semkova, J., Malchev, S., Tomov, B., Matviichuk, Y., Dimitrov, P., Koleva, R., Dachev, T., … Shurshakov, V. (2018). Fine Resolution Epithermal Neutron Detector (FREND) Onboard the ExoMars Trace Gas Orbiter. *Space Science Reviews*, *214*(5), 86. https://doi.org/10.1007/s11214-018-0522-5

Morgan, G. A., Putzig, N. E., Perry, M. R., Sizemore, H. G., Bramson, A. M., Petersen, E. I., Bain, Z. M., Baker, D. M. H., Mastrogiuseppe, M., Hoover, R. H., Smith, I. B., Pathare, A., Dundas, C. M., & Campbell, B. A. (2021). Availability of subsurface water-ice resources in the northern mid-latitudes of Mars. *Nature Astronomy*, 1–7. https://doi.org/10.1038/s41550-020-01290-z

Morgenstern, A., Hauber, E., Reiss, D., Gasselt, S. van, Grosse, G., & Schirrmeister, L. (2007). Deposition and degradation of a volatile-rich layer in Utopia Planitia and implications for climate history on Mars. *Journal of Geophysical Research: Planets*, *112*(E6). https://doi.org/10.1029/2006JE002869

Mouginot, J., Pommerol, A., Kofman, W., Beck, P., Schmitt, B., Herique, A., Grima, C., Safaeinili, A., & Plaut, J. J. (2010). The 3–5 MHz global reflectivity map of Mars by MARSIS/Mars Express: Implications for the current inventory of subsurface H2O. *Icarus*, *210*(2), 612–625. https://doi.org/10.1016/j.icarus.2010.07.003

Musselwhite, D. S., Swindle, T. D., & Lunine, J. I. (2001). Liquid CO2 breakout and the formation of recent small gullies on Mars. *Geophysical Research Letters*, *28*(7), 1283–1285. https://doi.org/10.1029/2000GL012496

Mustard, J. F., Cooper, C. D., & Rifkin, M. K. (2001). Evidence for recent climate change on Mars from the identification of youthful near-surface ground ice. *Nature*, *412*(6845), 411–414. https://doi.org/doi:10.1038/35086515

Mutch, T. A., Arvidson, R. E., Binder, A. B., Guinness, E. A., & Morris, E. C. (1977). The geology of the Viking Lander 2 site. *Journal of Geophysical Research*, *82*(28), 4452–4467. https://doi.org/10.1029/JS082i028p04452

Neukum, G., Jaumann, R., & the HRSC Co-Investigator and Experiment Team. (2004). HRSC: The high resolution stereo camera of Mars Express. *Mars Express: The Scientific*

Payload, *ESA Special Publication*, *SP-1240*, *Noordwijk*, *Netherlands: ESA Publications Division*, 17–35.

Paige, D. A. (1992). The thermal stability of near-surface ground ice on Mars. *Nature*, *356*(6364), 43–45. https://doi.org/10.1038/356043a0

Pathare, A. V., Feldman, W. C., Prettyman, T. H., & Maurice, S. (2018). Driven by excess? Climatic implications of new global mapping of near-surface water-equivalent hydrogen on Mars. *Icarus*, *301*, 97–116. https://doi.org/10.1016/j.icarus.2017.09.031

Pechmann, J. C. (1980). The origin of polygonal troughs on the Northern Plains of Mars. *Icarus*, *42*(2), 185–210. https://doi.org/10.1016/0019-1035(80)90071-8

Petersen, E. I., Holt, J. W., & Levy, J. S. (2018). High Ice Purity of Martian Lobate Debris Aprons at the Regional Scale: Evidence From an Orbital Radar Sounding Survey in Deuteronilus and Protonilus Mensae. *Geophysical Research Letters*, *45*(21), 11,595-11,604. https://doi.org/10.1029/2018GL079759

Picardi, G., Biccari, D., Seu, R., Plaut, J., Johnson, W. T. K., Jordan, R. L., Safaeinili, A., Gurnett, D. A., Huff, R., Orosei, R., Bombaci, O., Calabrese, D., & Zampolini, E. (2004). MARSIS: Mars Advanced Radar for Subsurface and Ionosphere Sounding. *Mars Express: The Scientific Payload*, *ESA Special Publication*, *SP-1240*, *Noordwijk*, *Netherlands: ESA Publications Division*, 51–69.

Pierce, T. L., & Crown, D. A. (2003). Morphologic and topographic analyses of debris aprons in the eastern Hellas region, Mars. *Icarus*, *163*(1), 46–65. https://doi.org/10.1016/S0019-1035(03)00046-0

Piqueux, S., Buz, J., Edwards, C. S., Bandfield, J. L., Kleinböhl, A., Kass, D. M., & Hayne, P. O. (2019). Widespread Shallow Water Ice on Mars at High Latitudes and Midlatitudes. *Geophysical Research Letters*, *46*(24), 14290–14298. https://doi.org/10.1029/2019GL083947

Plaut, J. J., Safaeinili, A., Holt, J. W., Phillips, R. J., Head, J. W., Seu, R., Putzig, N. E., & Frigeri, A. (2009). Radar evidence for ice in lobate debris aprons in the mid-northern latitudes of Mars. *Geophysical Research Letters*, *36*(2), L02203. https://doi.org/10.1029/2008GL036379

Putzig, N. E., Morgan, G. A., Sizemore, H. G., Baker, D. M. H., Petersen, E. I., Pathare, A. V., Dundas, C. M., Bramson, A. M., Courville, S. W., Perry, M. R., Nerozzi, S., Bain, Z. M., Hoover, R. H., Campbell, B. A., Mastrogiuseppe, M., Mellon, M. T., Seu, R., & Smith, I. B. (Submitted). Ice Resource Mapping on Mars. In V. Badescu, K. Zacny, & Y. Bar-Cohen (Eds.), *Handbook of Space Resources*. Springer Nature.

Ramohalli, K., Dowler, W., French, J., & Ash, R. (1987). Some aspects of space propulsion with extraterrestrial resources. *Journal of Spacecraft and Rockets*, *24*(3), 236–244. https://doi.org/10.2514/3.25905

Reiss, D., & Jaumann, R. (2003). Recent debris flows on Mars: Seasonal observations of the Russell Crater dune field. *Geophysical Research Letters*, *30*(6). https://doi.org/10.1029/2002GL016704

Rossbacher, L. A., & Judson, S. (1981). Ground ice on Mars: Inventory, distribution, and resulting landforms. *Icarus*, *45*(1), 39–59. https://doi.org/10.1016/0019-1035(81)90005-1

Sagan, C., Veverka, J., Fox, P., Dubisch, R., Lederberg, J., Levinthal, E., Quam, L., Tucker, R., Pollack, J. B., & Smith, B. A. (1972). Variable features on Mars: Preliminary mariner 9 television results. *Icarus*, *17*(2), 346–372. https://doi.org/10.1016/0019-1035(72)90005-X

Salisbury, J. W. (1966). The light and dark areas of Mars. *Icarus*, *5*(1), 291–298. https://doi.org/10.1016/0019-1035(66)90039-X

Schon, S. C., Head, J. W., & Fassett, C. I. (2012). Recent high-latitude resurfacing by a climate-related latitude-dependent mantle: Constraining age of emplacement from counts of small craters. *Planetary and Space Science*, *69*(1), 49–61. https://doi.org/10.1016/j.pss.2012.03.015

Schon, S. C., Head, J. W., & Milliken, R. E. (2009). A recent ice age on Mars: Evidence for climate oscillations from regional layering in mid-latitude mantling deposits. *Geophysical Research Letters*, *36*(15), L15202. https://doi.org/10.1029/2009GL038554

Schorghofer, N., & Aharonson, O. (2005). Stability and exchange of subsurface ice on Mars. *Journal of Geophysical Research: Planets*, *110*(E5), E05003. https://doi.org/10.1029/2004JE002350

Seibert, N. M., & Kargel, J. S. (2001). Small-scale Martian polygonal terrain: Implications for liquid surface water. *Geophysical Research Letters*, *28*(5), 899–902. https://doi.org/10.1029/2000GL012093

Séjourné, A., Costard, F., Gargani, J., Soare, R. J., Fedorov, A., & Marmo, C. (2011). Scalloped depressions and small-sized polygons in western Utopia Planitia, Mars: A new formation hypothesis. *Planetary and Space Science*, *59*(5), 412–422. https://doi.org/10.1016/j.pss.2011.01.007

Seu, R., Phillips, R. J., Biccari, D., Orosei, R., Masdea, A., Picardi, G., Safaeinili, A., Campbell, B. A., Plaut, J. J., Marinangeli, L., Smrekar, S. E., & Nunes, D. C. (2007). SHARAD sounding radar on the Mars Reconnaissance Orbiter. *Journal of Geophysical Research: Planets*, *112*(E5). https://doi.org/10.1029/2006JE002745

Sharp, R. P. (1973). Mars: Fretted and chaotic terrains. *Journal of Geophysical Research*, *78*(20), 4073–4083. https://doi.org/10.1029/JB078i020p04073

Shean, D. E., Head, J. W., Fastook, J. L., & Marchant, D. R. (2007). Recent glaciation at high elevations on Arsia Mons, Mars: Implications for the formation and evolution of large tropical mountain glaciers. *Journal of Geophysical Research: Planets*, *112*(E3), E03004. https://doi.org/10.1029/2006JE002761

Shean, D. E., Head, J. W., & Marchant, D. R. (2005). Origin and evolution of a cold-based tropical mountain glacier on Mars: The Pavonis Mons fan-shaped deposit. *Journal of Geophysical Research: Planets*, *110*(E5), E05001. https://doi.org/10.1029/2004JE002360

Smith, D. E., Zuber, M. T., Frey, H. V., Garvin, J. B., Head, J. W., Muhleman, D. O., Pettengill, G. H., Phillips, R. J., Solomon, S. C., Zwally, H. J., Banerdt, W. B., Duxbury, T. C., Golombek, M. P., Lemoine, F. G., Neumann, G. A., Rowlands, D. D., Aharonson, O., Ford, P. G., Ivanov, A. B., … Sun, X. (2001). Mars Orbiter Laser Altimeter: Experiment summary after the first year of global mapping of Mars. *Journal of Geophysical Research: Planets*, *106*(E10), 23689–23722. https://doi.org/10.1029/2000JE001364

Smith, I. B., Putzig, N. E., Holt, J. W., & Phillips, R. J. (2016). An ice age recorded in the polar deposits of Mars. *Science*, *352*(6289), 1075–1078. https://doi.org/10.1126/science.aad6968

Smith, P. H., Tamppari, L. K., Arvidson, R. E., Bass, D., Blaney, D., Boynton, W. V., Carswell, A., Catling, D. C., Clark, B. C., Duck, T., DeJong, E., Fisher, D., Goetz, W., Gunnlaugsson, H. P., Hecht, M. H., Hipkin, V., Hoffman, J., Hviid, S. F., Keller, H. U., … Zent, A. P. (2009). H2O at the Phoenix Landing Site. *Science*, *325*(5936), 58–61. https://doi.org/10.1126/science.1172339

Snyder, C. W. (1979). The planet Mars as seen at the end of the Viking Mission. *Journal of Geophysical Research: Solid Earth*, *84*(B14), 8487–8519. https://doi.org/10.1029/JB084iB14p08487

Soare, R. J., Osinski, G. R., & Roehm, C. L. (2008). Thermokarst lakes and ponds on Mars in the very recent (late Amazonian) past. *Earth and Planetary Science Letters*, *272*(1), 382–393. https://doi.org/10.1016/j.epsl.2008.05.010

Soderblom, L. A., Kreidler, T. J., & Masursky, H. (1973). Latitudinal distribution of a debris mantle on the Martian surface. *Journal of Geophysical Research*, *78*(20), 4117–4122. https://doi.org/10.1029/JB078i020p04117

Souness, C., Hubbard, B., Milliken, R. E., & Quincey, D. (2012). An inventory and population-scale analysis of martian glacier-like forms. *Icarus*, *217*(1), 243–255. https://doi.org/10.1016/j.icarus.2011.10.020

Souness, C. J., & Hubbard, B. (2013). An alternative interpretation of late Amazonian ice flow: Protonilus Mensae, Mars. *Icarus*, *225*(1), 495–505. https://doi.org/10.1016/j.icarus.2013.03.030

Squyres, S. W. (1978). Martian Fretted Terrain: Flow of Erosional Debris. *Icarus*, *34*, 600–613. https://doi.org/10.1016/0019-1035(78)90048-9

Squyres, S. W. (1979). The distribution of lobate debris aprons and similar flows on Mars. *Journal of Geophysical Research: Solid Earth*, *84*(B14), 8087–8096. https://doi.org/10.1029/JB084iB14p08087

Squyres, S. W., & Carr, M. H. (1986). Geomorphic evidence for the distribution of ground ice on Mars. *Science (New York, N.Y.)*, *231*(4735), 249–252. https://doi.org/10.1126/science.231.4735.249

Strughold, H. (1967). Synopsis of Martian Life Theories. In F. I. Ordway (Ed.), *Advances in Space Science and Technology* (Vol. 9, pp. 105–122). Elsevier. https://doi.org/10.1016/B978-1-4831-9967-2.50008-5

Stuurman, C. M., Osinski, G. R., Holt, J. W., Levy, J. S., Brothers, T. C., Kerrigan, M., & Campbell, B. A. (2016). SHARAD detection and characterization of subsurface water

ice deposits in Utopia Planitia, Mars. *Geophysical Research Letters*, *43*(18), 9484–9491. https://doi.org/10.1002/2016GL070138

Touma, J., & Wisdom, J. (1993). The Chaotic Obliquity of Mars. *Science*, *259*(5099), 1294–1297. https://doi.org/10.1126/science.259.5099.1294

Vincendon, M., Mustard, J., Forget, F., Kreslavsky, M., Spiga, A., Murchie, S., & Bibring, J.-P. (2010). Near-tropical subsurface ice on Mars. *Geophysical Research Letters*, *37*(1). https://doi.org/10.1029/2009GL041426

Viola, D., & McEwen, A. S. (2018). Geomorphological Evidence for Shallow Ice in the Southern Hemisphere of Mars. *Journal of Geophysical Research: Planets*, *123*(1), 262–277. https://doi.org/10.1002/2017JE005366

Viola, D., McEwen, A. S., Dundas, C. M., & Byrne, S. (2015). Expanded secondary craters in the Arcadia Planitia region, Mars: Evidence for tens of Myr-old shallow subsurface ice. *Icarus*, *248*, 190–204. https://doi.org/10.1016/j.icarus.2014.10.032

Warner, N. H., Gupta, S., Calef, F., Grindrod, P., Boll, N., & Goddard, K. (2015). Minimum effective area for high resolution crater counting of martian terrains. *Icarus*, *245*, 198–240. https://doi.org/10.1016/j.icarus.2014.09.024

Zanetti, M., Hiesinger, H., Reiss, D., Hauber, E., & Neukum, G. (2010). Distribution and evolution of scalloped terrain in the southern hemisphere, Mars. *Icarus*, *206*(2), 691–706. https://doi.org/10.1016/j.icarus.2009.09.010